Imaging: Photodiodes

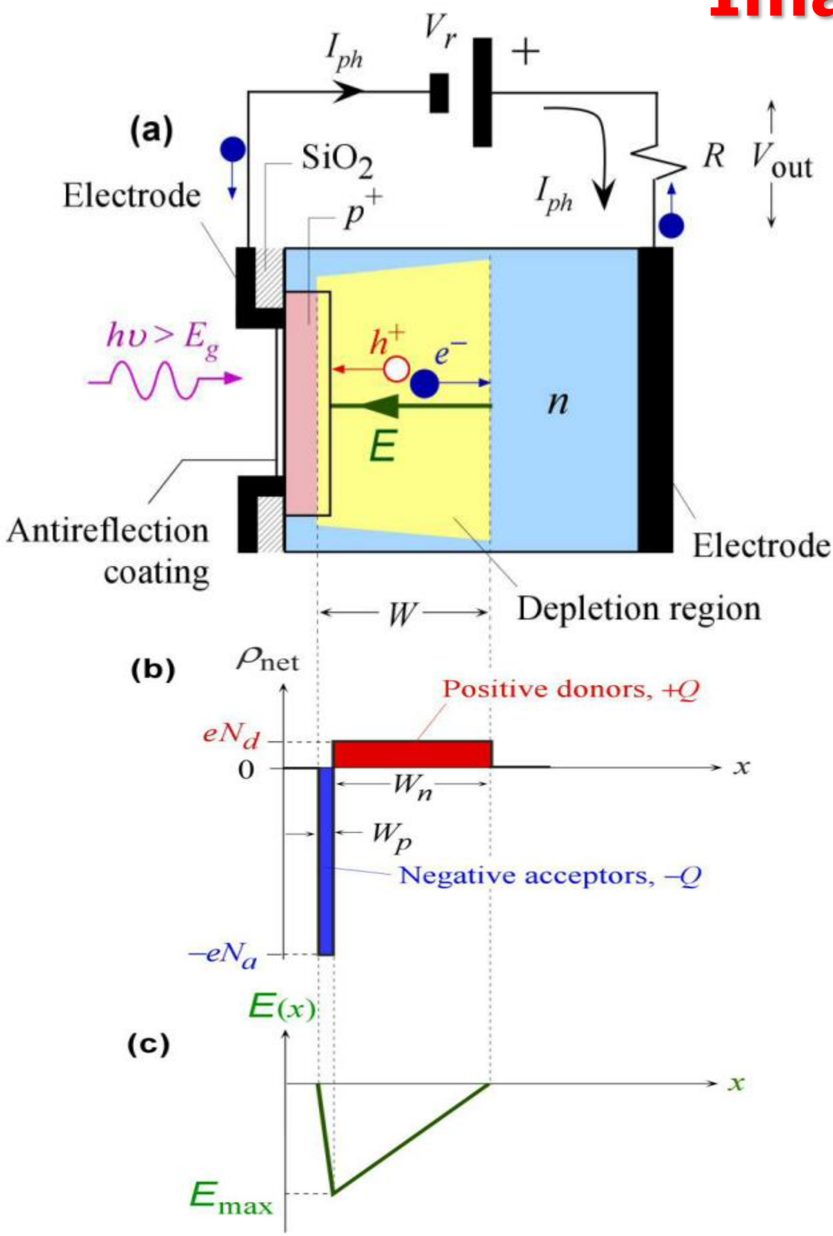

Reverse-biased *pn* junction photodiode

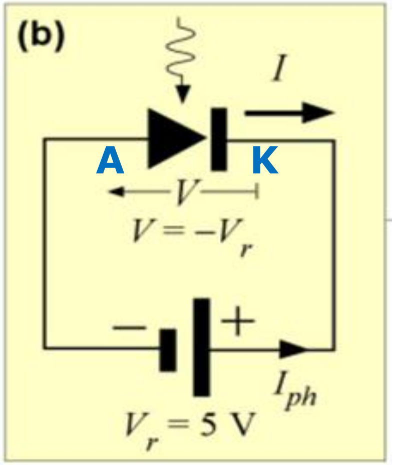

← Space charge and electric field

N_d , N_a = donor and acceptor concentrations
E_g = energy gap between valence and conduction bands

S.O. Kasap, *Optoelectronics and Photonics: Principles and Practices,* © Pearson Education

Photodiodes

Absorption depth (typ. a few / few tens microns): distance at which the light drops by a factor *1/e*

E-H pairs generated in neutral regions diffuse in material

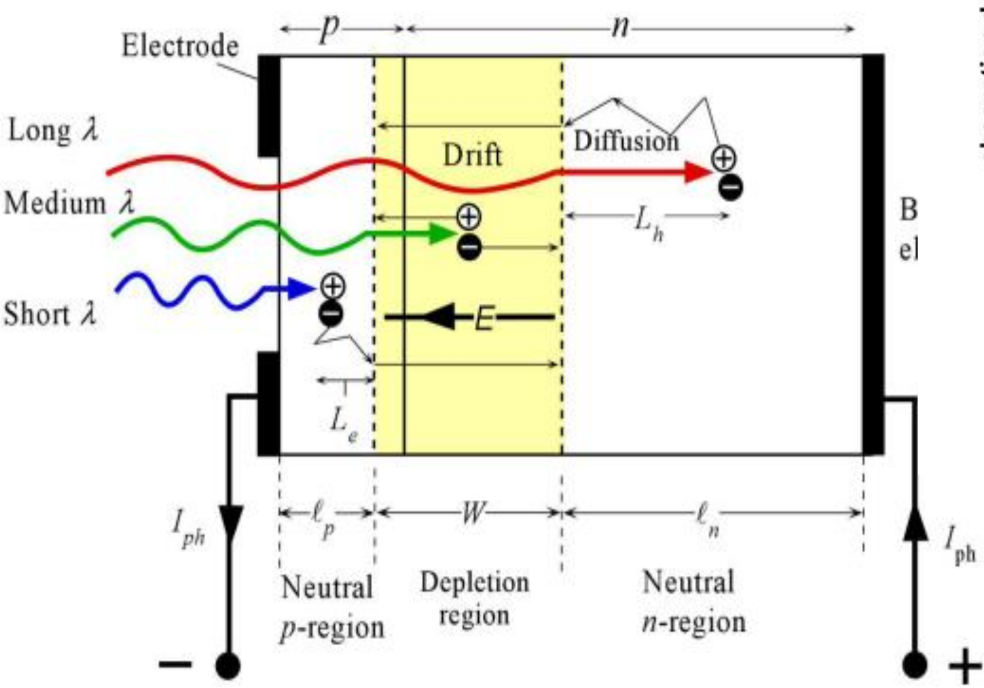

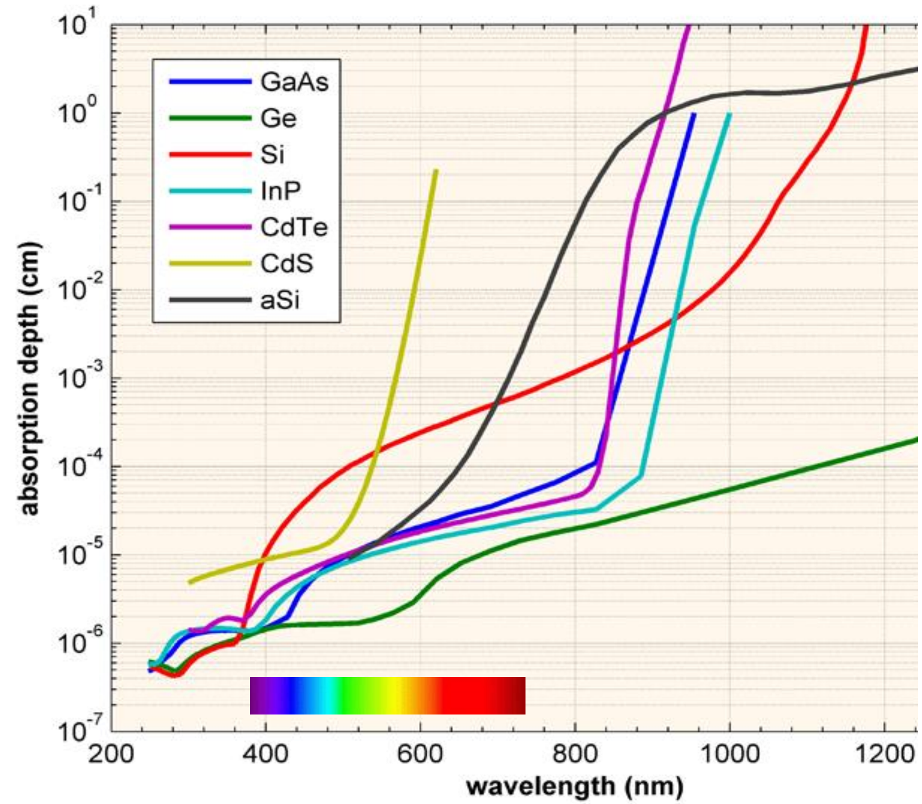

S.O. Kasap, *Optoelectronics and Photonics: Principles and Practices*, © Pearson Education

Photodiodes

pn junction, reverse biased; photogeneration inside depletion region and inside neutral region

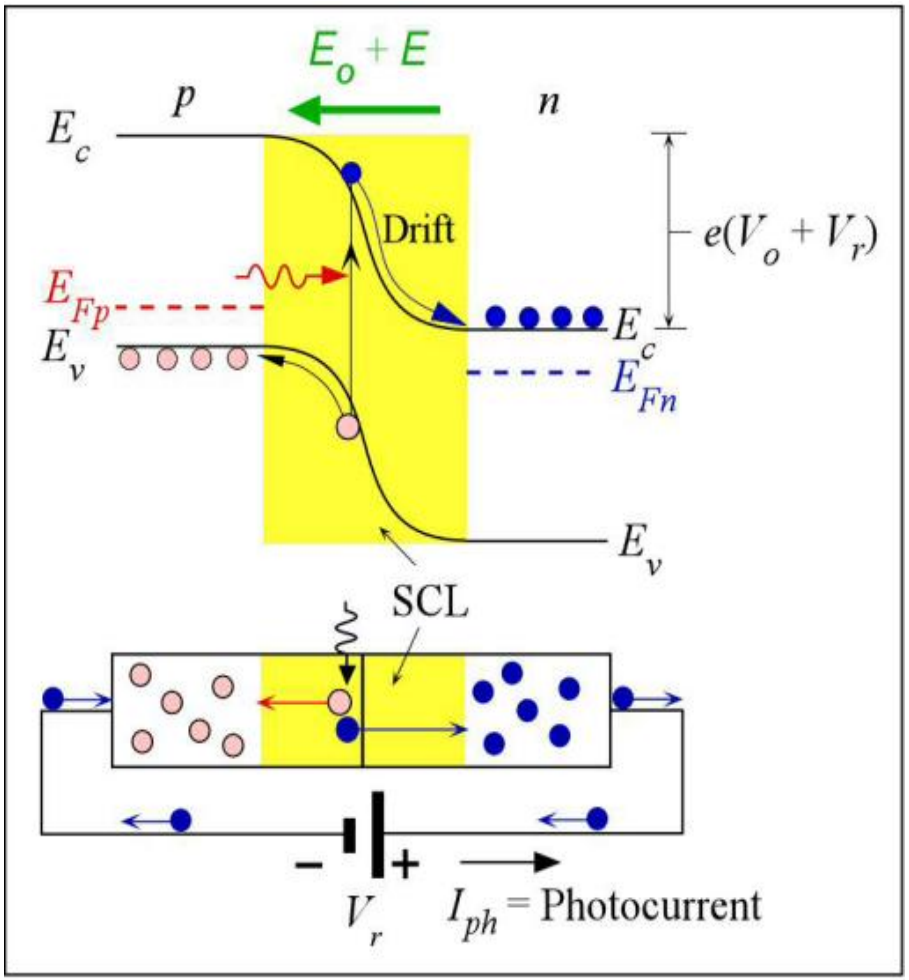

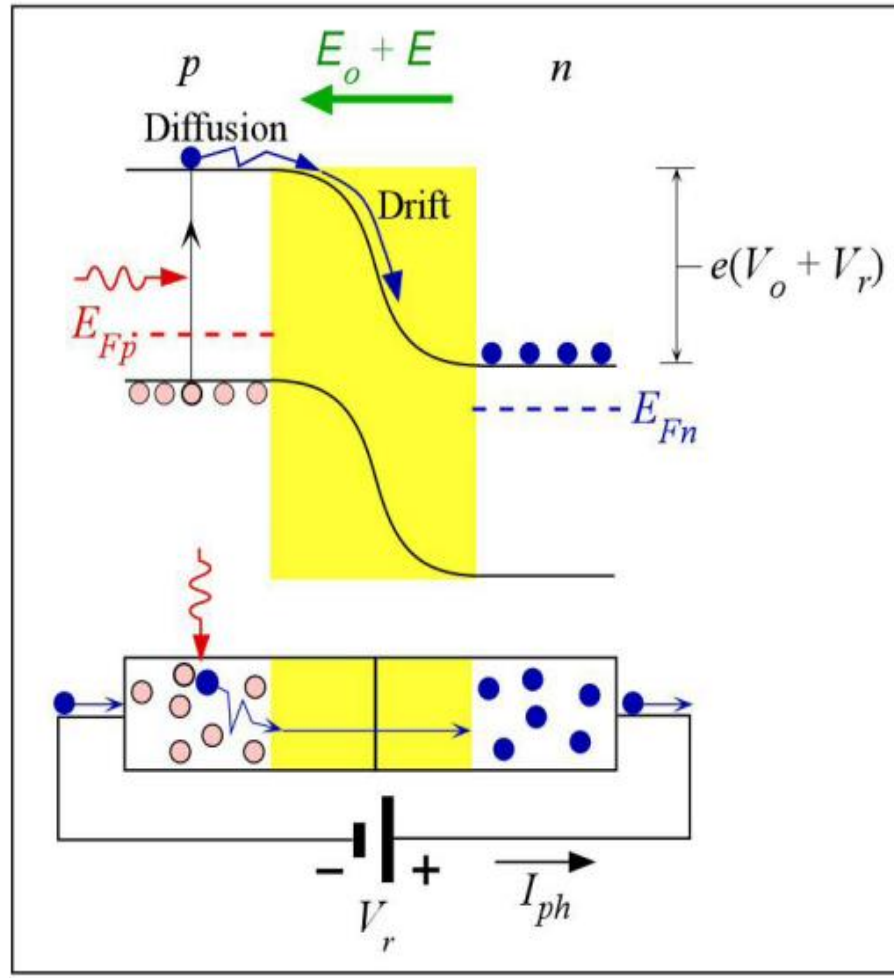

Photodiodes

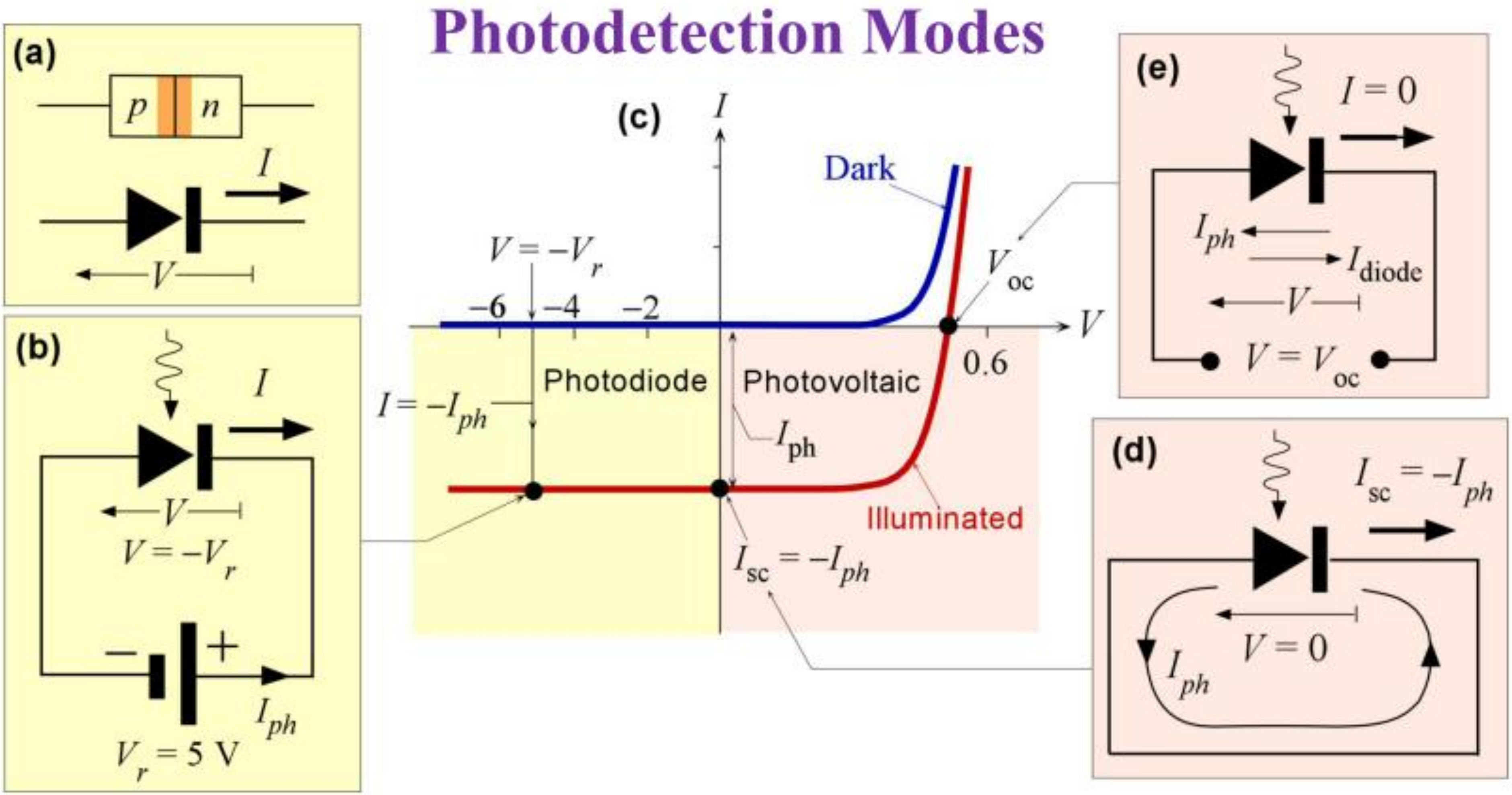

S.O. Kasap, *Optoelectronics and Photonics: Principles and Practices,* © Pearson Education

Photodiodes

The number of collected charges is

- linearly dependent on light level and exposure time and
- nonlinearly dependent on wavelength

$$I_{ph} = q\ \eta\ P_0 / h\nu \qquad [C \times W / J = C / s = A]$$

q	elementary charge
$\eta = \eta(\lambda)$	*external quantum efficiency (QE)* (collected EH pairs / incident photons) (see curves in datasheet)
P_0	power of incident light
h	Planck's constant
$\nu = c / \lambda$	frequency

} $h\nu$ = light energy

Photodiode circuits

Basic circuit and the *load line* $(V_r = 6V, R_L = 1\ M\Omega)$

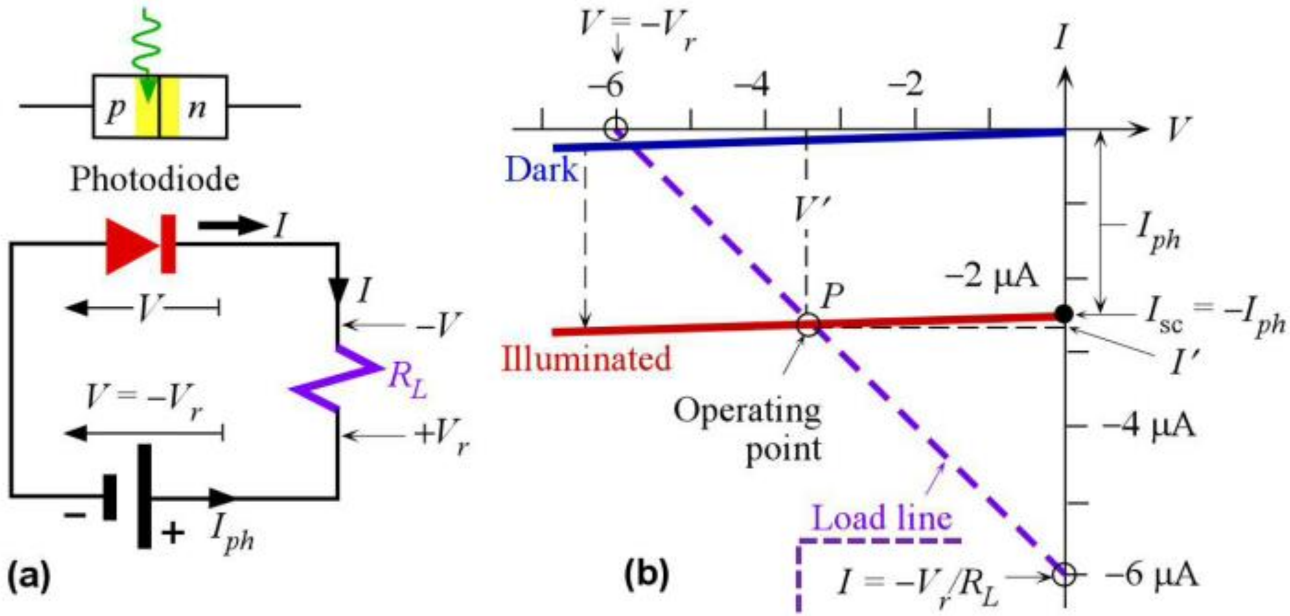

P is the operating point

$V' = -3.5$ V

$I' = -2.5$ μA

$I' \approx I_{ph}$

The current through R_L is

$$I = -(V + V_r)/R_L$$

Photodiode circuits

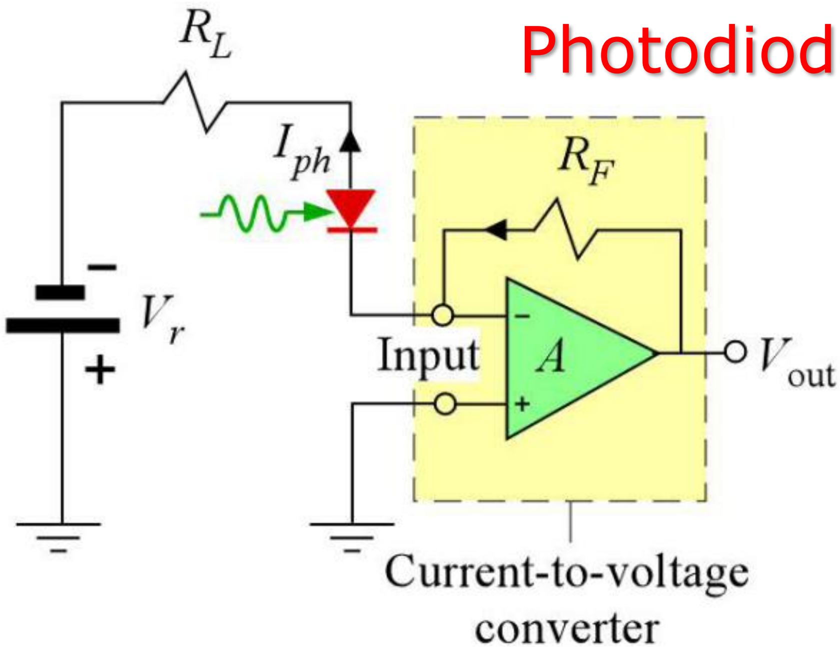

Principle of transimpedance amplifier (CCVS), $V_{out} = R_F\, I_{ph}$

Frequency response

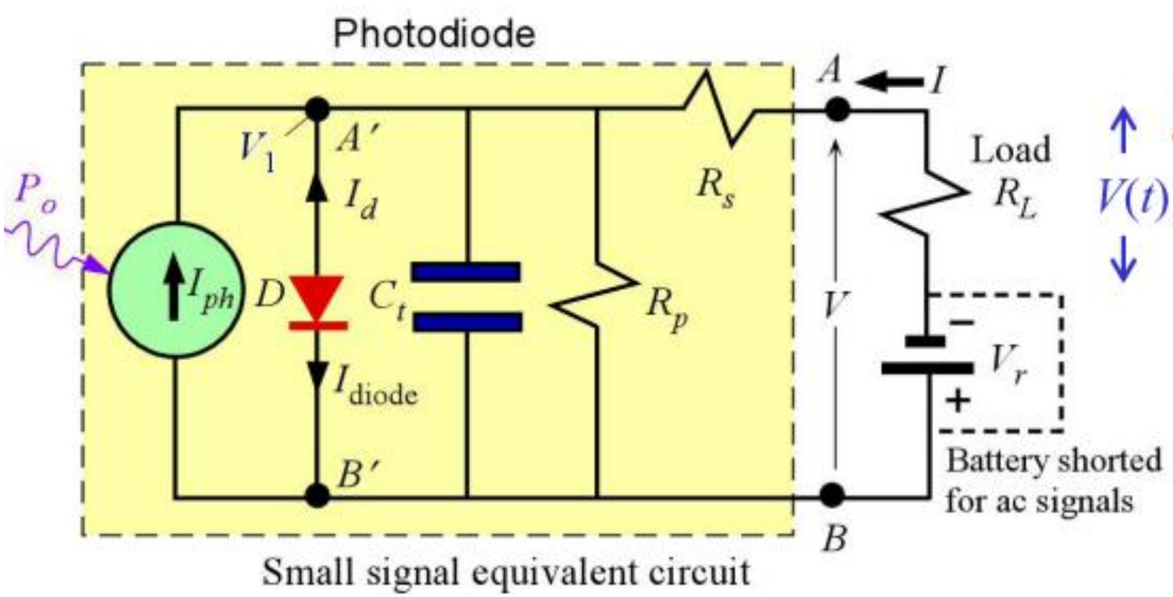

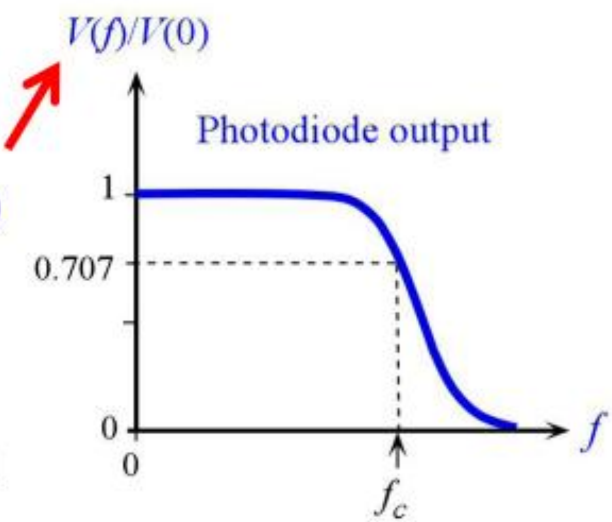

S.O. Kasap, *Optoelectronics and Photonics: Principles and Practices,* © Pearson Education

Image sensors

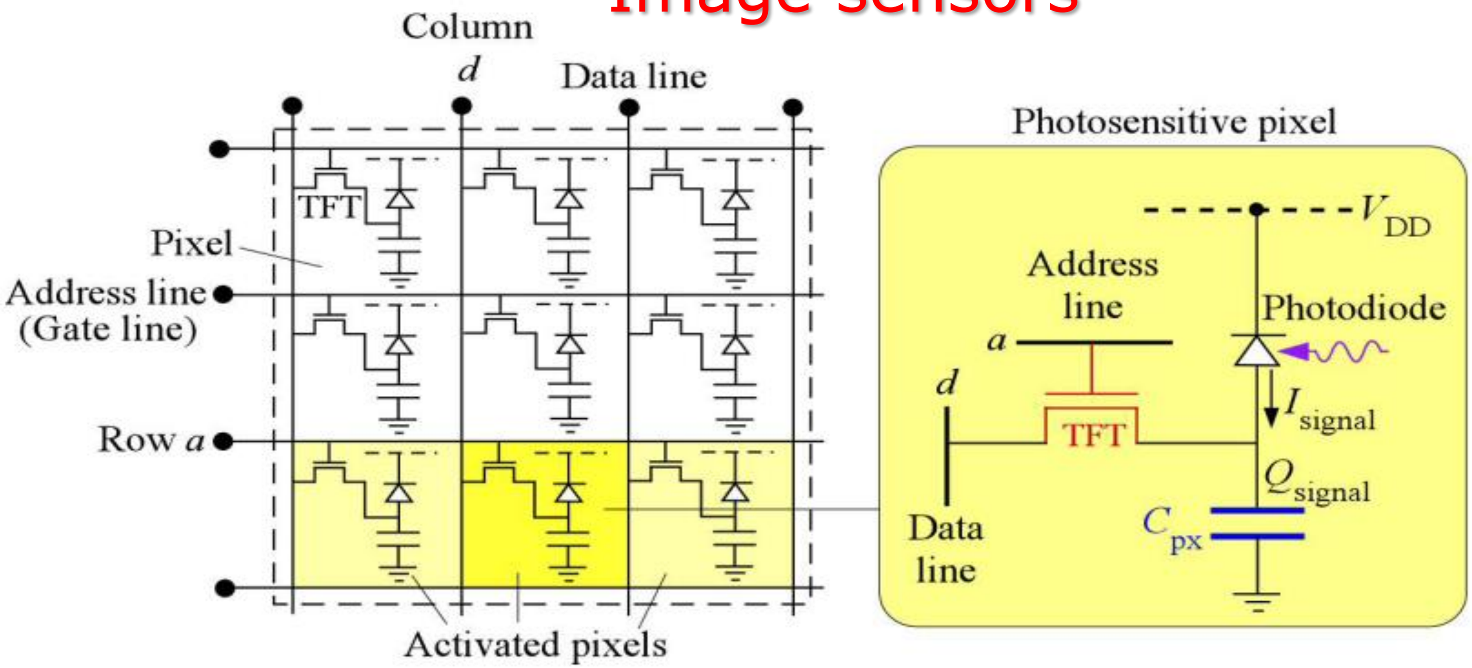

Active matrix addressing

Color acquisition

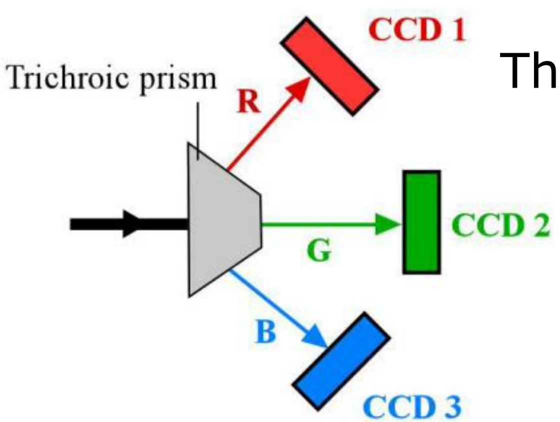

Three sensors

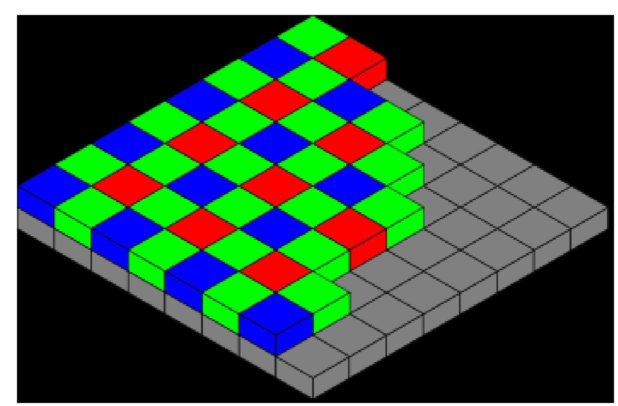

Single sensor +
RGB ***Bayer*** filter +
interpolation

S.O. Kasap, *Optoelectronics and Photonics: Principles and Practices*, © Pearson Education

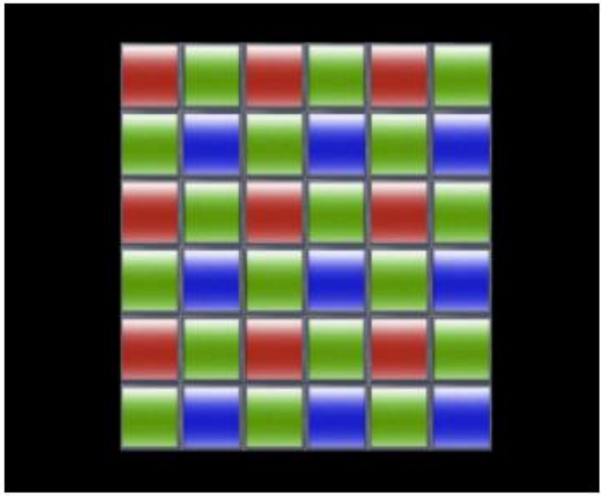

Repeating pattern in an array of 2 x 2 pixel units.

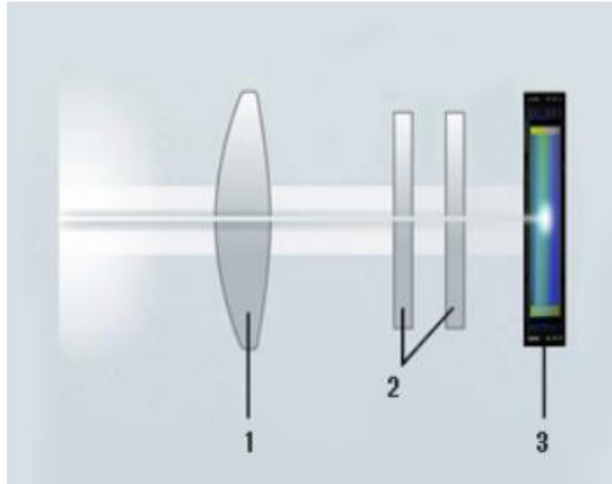

Lens with optical low-pass filters

1. Lens
2. Optical low-pass filter
3. Sensor

https://fujifilm-x.com/global/products/x-trans-cmos/

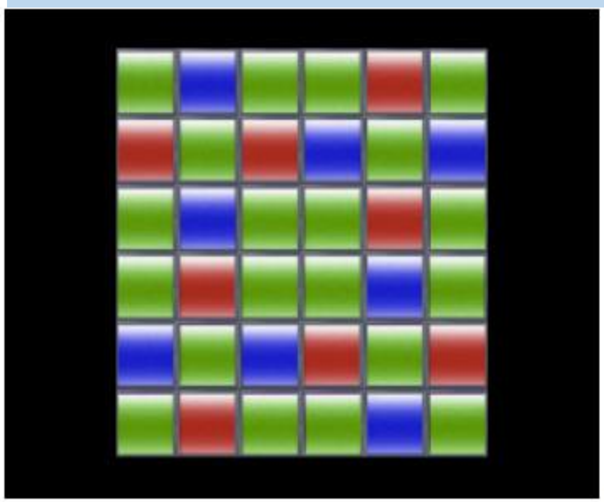

X-Trans filter (Fuji)

PROs

Higher degree of randomness with an array of 6 x 6 pixel units.

Without using an optical low-pass filter, Moiré and false colours are eliminated while realizing high resolution.

CONs

increased processing requirements

Work in progress: **Quantum Dots** (see paper)

CCD image sensors

Willard Boyle and George Smith, formerly of Bell Telephone Laboratories, in Murray Hill, N.J., shared the 2009 Nobel Prize in Physics for their invention of the **charge-coupled device (CCD)**, the basis for digital imagery

Photo: Alcatel-Lucent/Bell Labs

Camera Men: Willard Boyle [left] and George Smith [right] in 1970.

CCD image sensors

Electrons generated by each photodiode are sequentially carried along a set of **CCD shift registers** towards a charge-to-voltage converter (sort of CCVS)

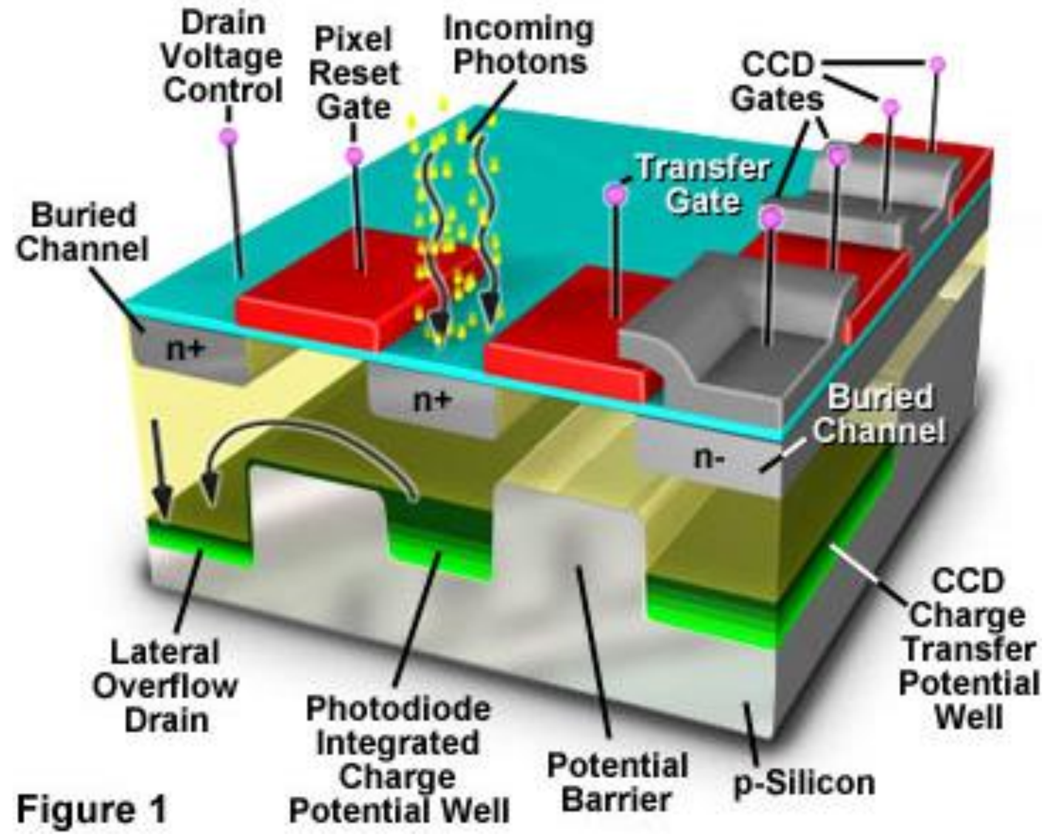

hamamatsu.magnet.fsu.edu/articles/ccdanatomy.html

Register input + one cell of a *buried-channel* CCD (higher transfer efficiency, easy charge transfer from ph.diode)

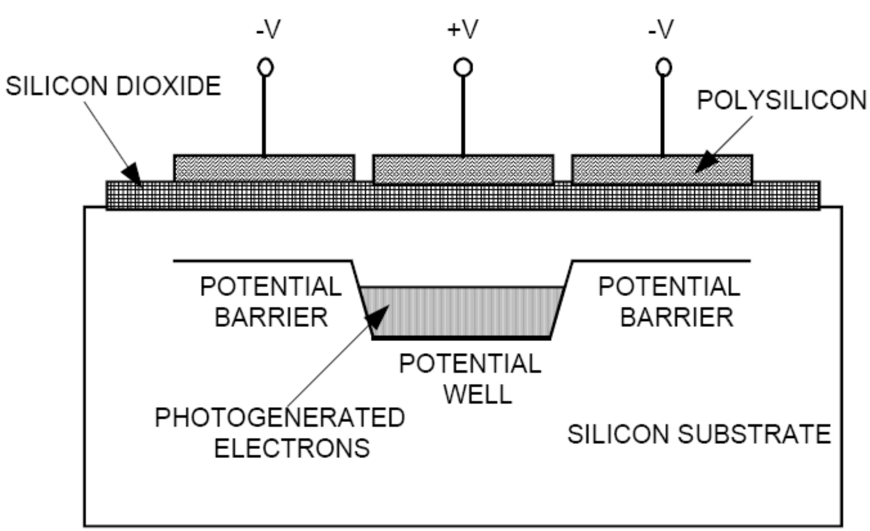

One register cell in a basic *surface-channel* CCD

CCD image sensors

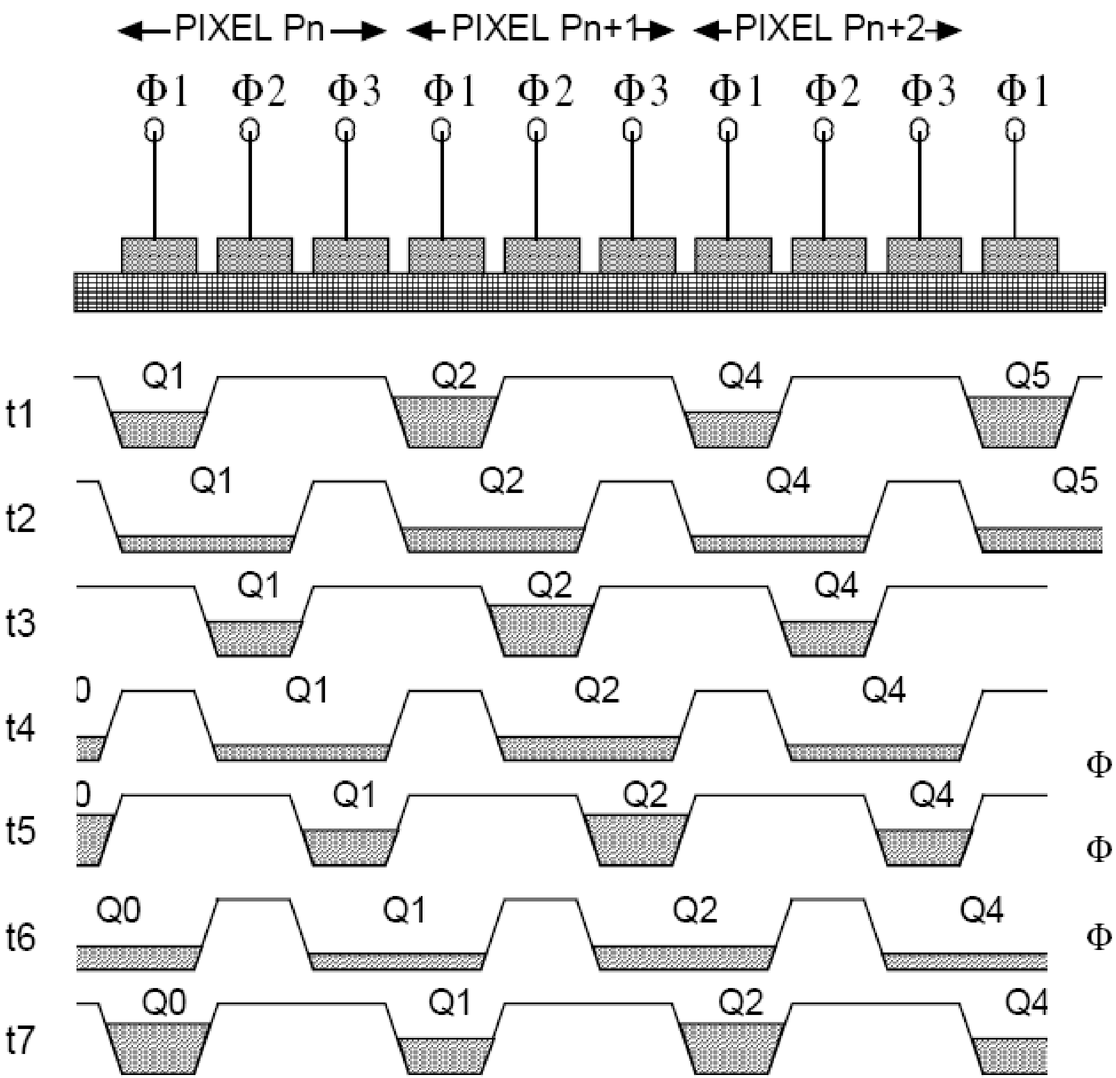

3-phase CCD

DIRECTION OF TRANSFER →

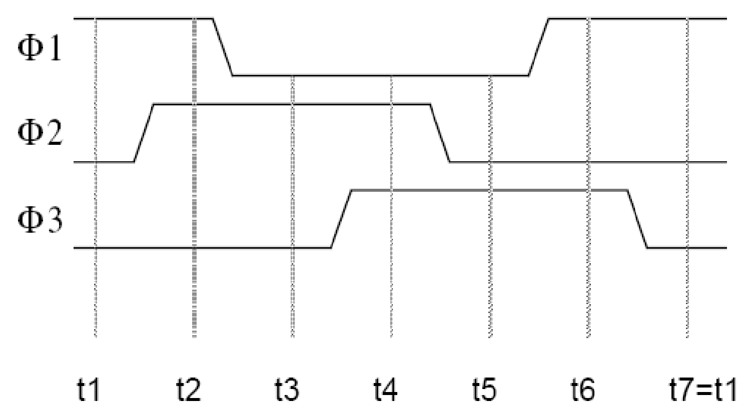

CCD image sensors

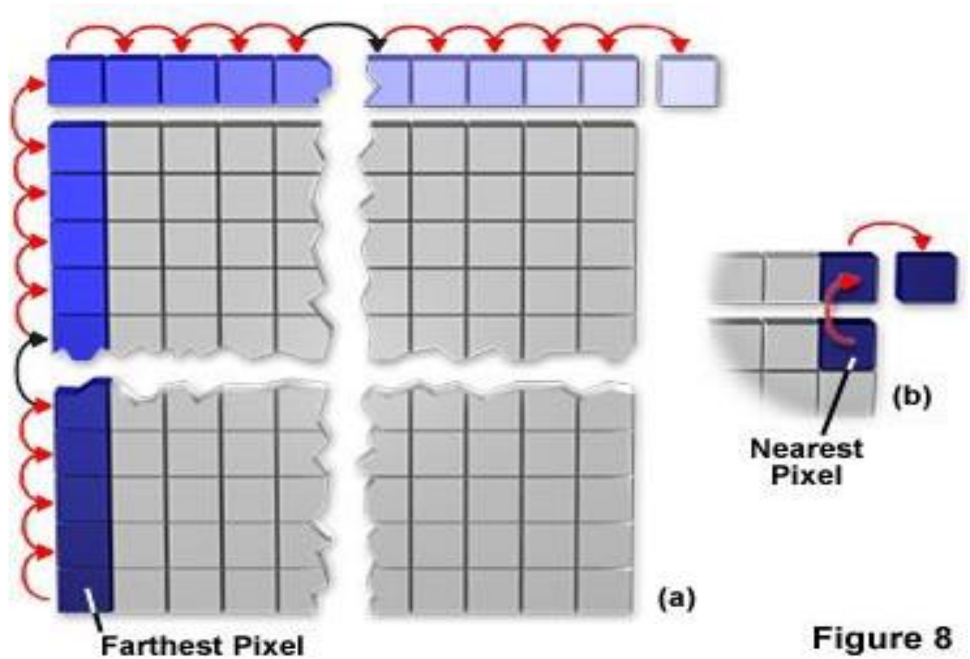

Problems:

- Dark current
- Transfer efficiency

e.g.: 99.9% single-transfer efficiency, HD frame size

$0.999 \wedge (1080+1920) = 0.0497$

→ 5% global efficiency for the farthest pixel

Actual efficiencies are above 0.999995

CCD architectures

Full-frame: nearly 100% of surface is photosensitive. Must be protected from light during readout, by an electromechanical shutter.

- slow (bottleneck is serial register)
- (beware: in photography slang, full-frame = size of old "35mm" film, 36x24 mm)

Frame-transfer: one-half covered with an opaque mask and used as a buffer. Fast (new exposure and readout of previous frame simultaneous). Shutter not needed

Interline-transfer: fast transfer to masked CCD. Shutter not needed

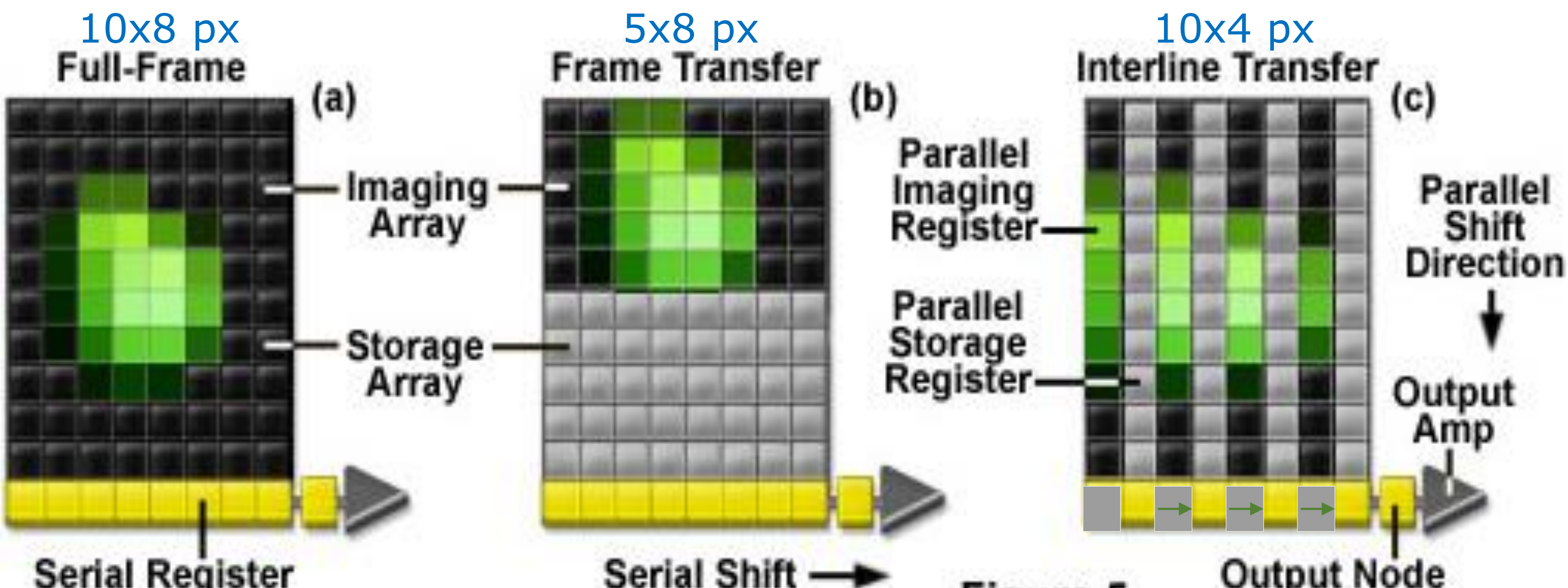

CCD architectures

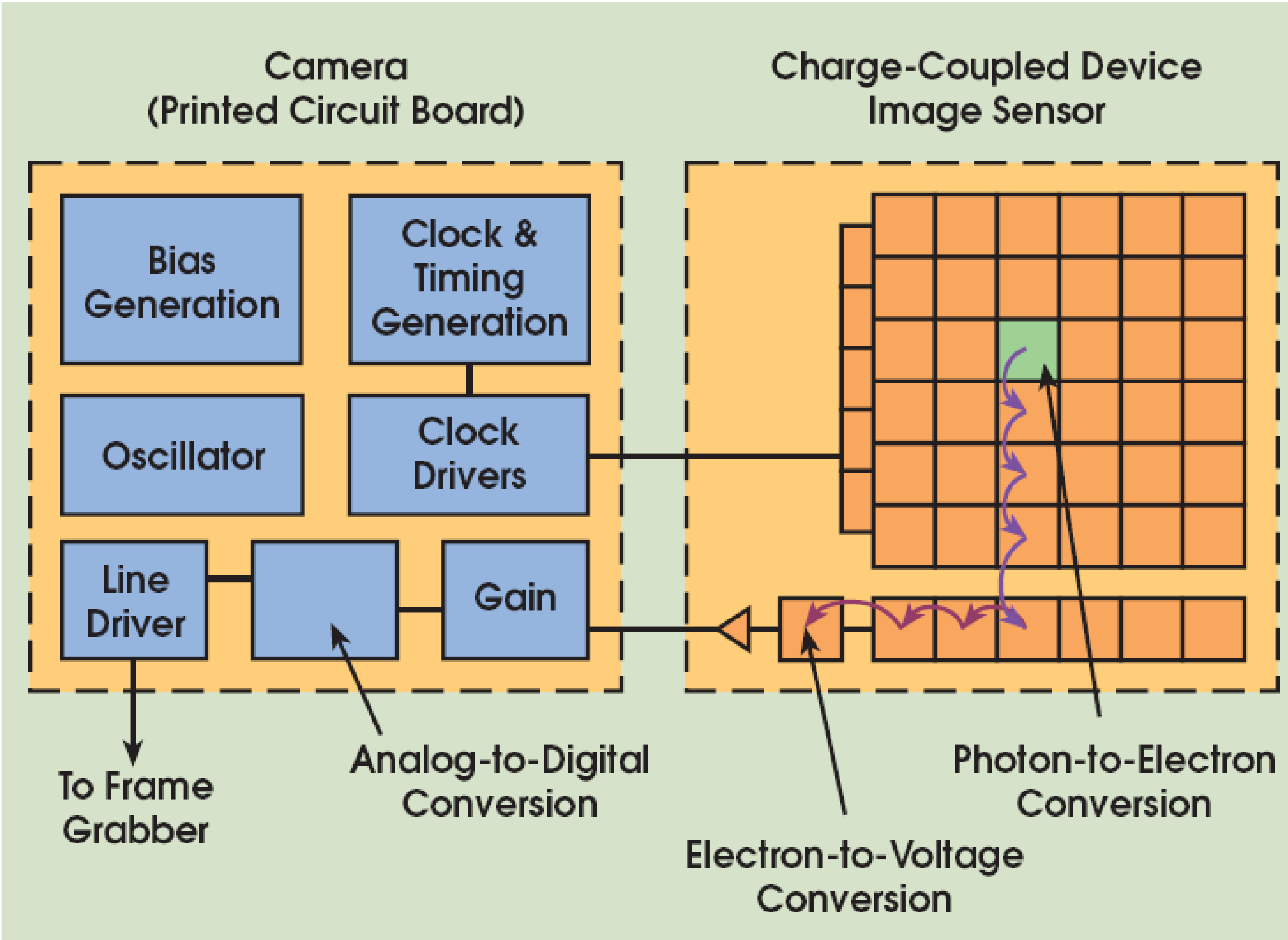

CMOS image sensor

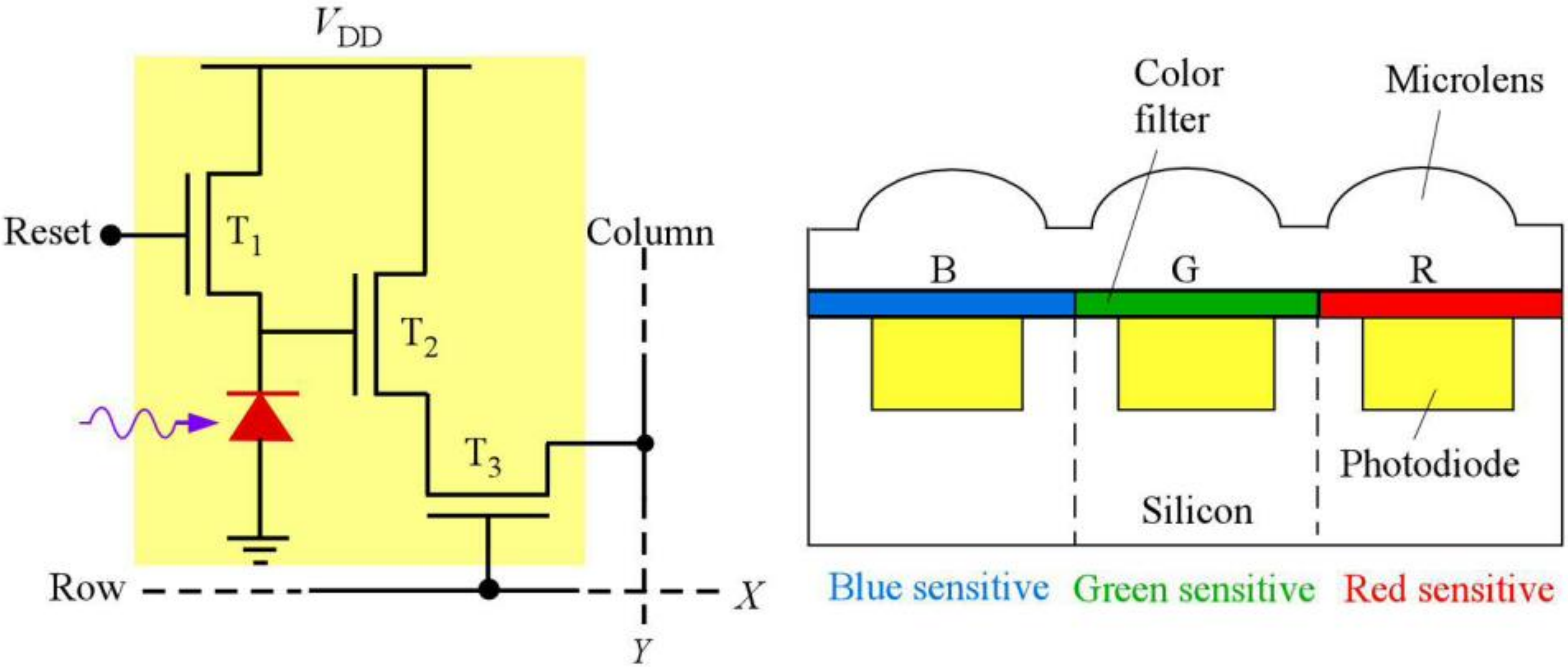

CMOS architecture

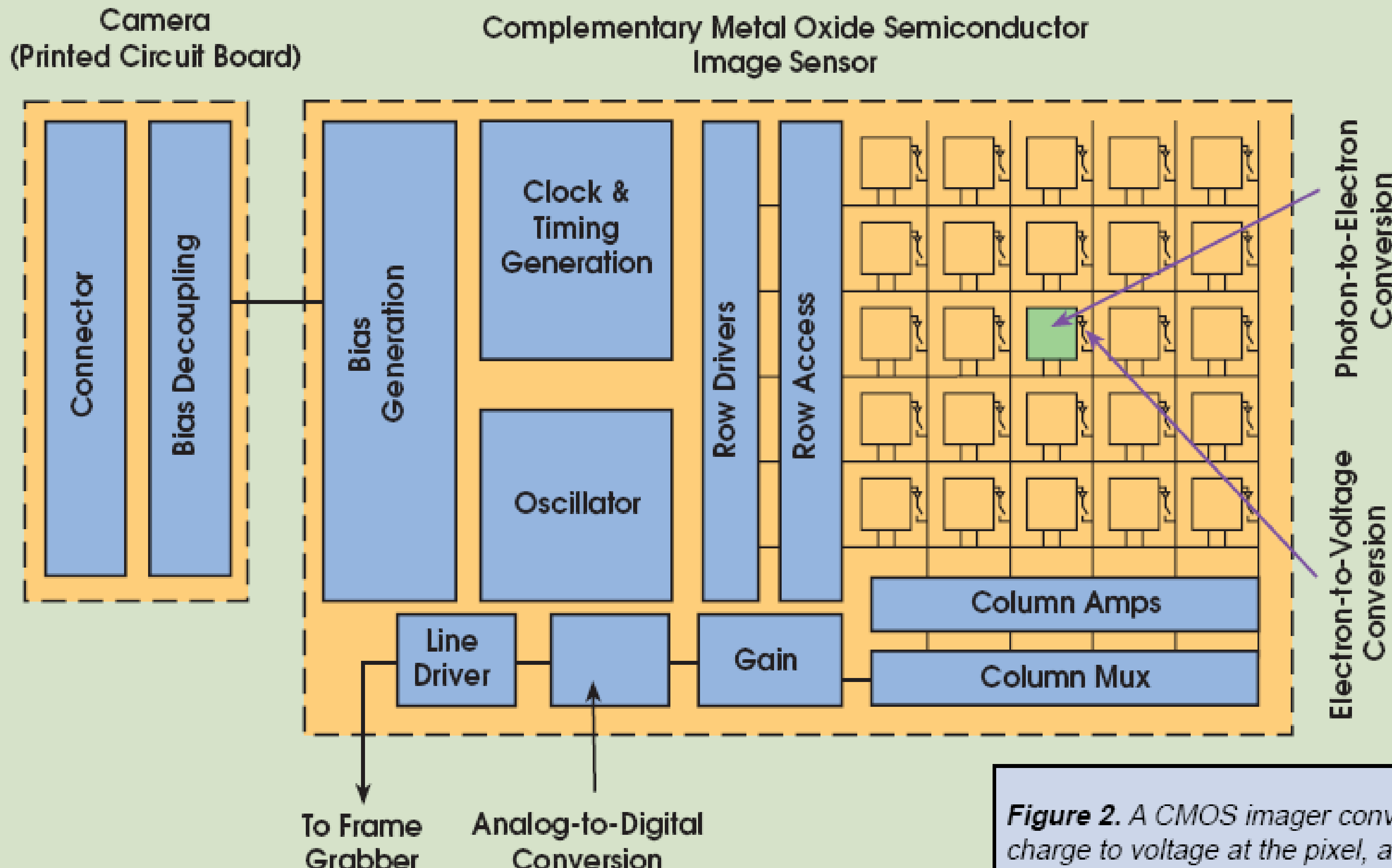

Figure 2. *A CMOS imager converts charge to voltage at the pixel, and most functions are integrated into the*

"Fixed pattern" noise

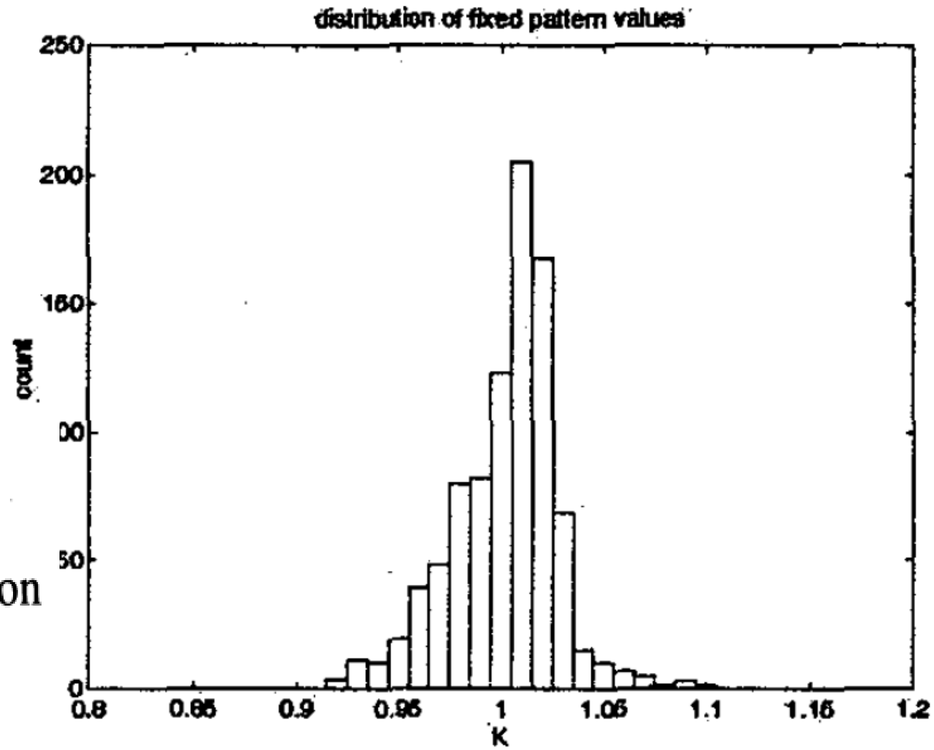

A problem,

Proceedings of the 2004 IEEE
International Conference on Robotics & Automation
New Orleans, LA • April 2004

Radiometric Calibration of CCD Sensors: Dark Current and Fixed Pattern Noise Estimation

Alberto Ortiz and Gabriel Oliver
Department of Mathematics and Computer Science
University of the Balearic Islands
Email: alberto.ortiz@uib.es, goliver@uib.es

an opportunity (forensic applic.),

IEEE TRANSACTIONS ON INFORMATION FORENSICS AND SECURITY, VOL. 1, NO. 2, JUNE 2006

Digital Camera Identification From Sensor Pattern Noise

Jan Lukáš, Jessica Fridrich, *Member, IEEE*, and Miroslav Goljan

…and further problems

IEEE Access
Multidisciplinary | Rapid Review | Open Access Journal

Received February 9, 2021, accepted March 24, 2021, date of publication April 1, 2021, date of current version April 12, 2021.
Digital Object Identifier 10.1109/ACCESS.2021.3070478

A Leak in PRNU Based Source Identification—Questioning Fingerprint Uniqueness

MASSIMO IULIANI[1,2], MARCO FONTANI[3], (Member, IEEE), AND ALESSANDRO PIVA[1,2], (Fellow, IEEE)
[1]Department of Information Engineering, University of Florence, 50139 Florence, Italy
[2]FORLAB—Multimedia Forensics Laboratory, 59100 Prato, Italy
[3]Amped Software, 34149 Trieste, Italy

Industrial applications: datasheets

HAMAMATSU
PHOTON IS OUR BUSINESS

Hamamatsu Photodiode Technical Information

ON Semiconductor®

KAF-50100 IMAGE SENSOR
8176(H) X 6132 (V) FULL FRAME CCD IMAGE SENSOR

PYTHON 25K/16K/12K/10K
Global Shutter CMOS Image Sensors

On Semiconductor is a spinoff from Motorola (1999). In 2014 they bought TrueSense Inc. that was a spinoff from Kodak (2012)

See also: EM_CCD - Electron Multiplying CCD Cameras

High-Dynamic-Range (**HDR**) sensors - CMOS

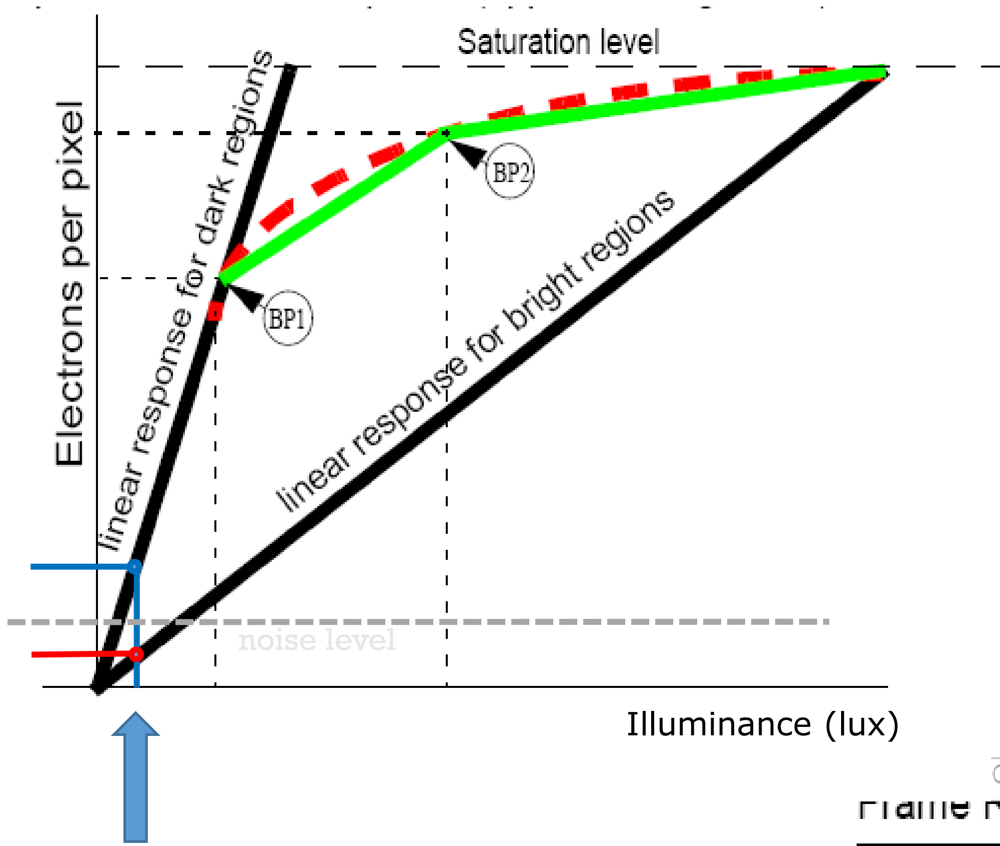

Higher slope of response → even in low-illuminance parts of the scene an acceptable SNR is achieved

y Specifications

y Format	Total: 664H x 504V Active: 648H x 488V
ctive Image Area	Total: 4.98mm x 3.78 mm Active: 4.86 mm x 3.66 mm
Optical Format	1/3"
Frame Rate	30 frames per second
Dynamic Range	62dB in linear mode 110dB in non linear mode
Electronic Shutter	Rolling reset
FPN	0.1%

HDR imaging with multiple **same-time** acquisitions

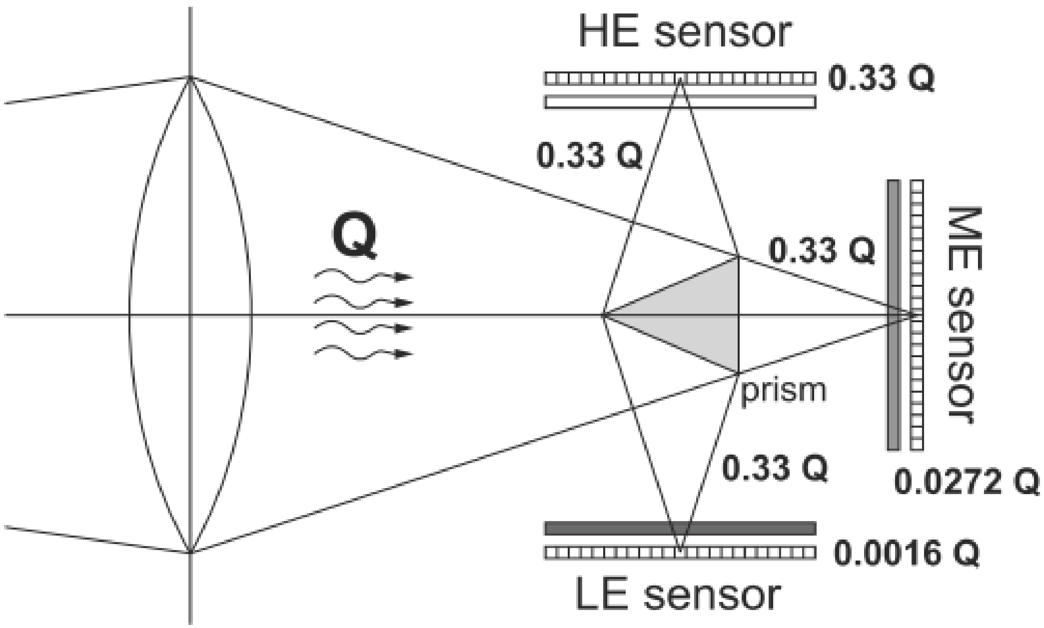

[Tocci11]

HE, ME, LE:
High-, Medium-, Low-Exposure sensors

Figure 2: A traditional beamsplitting HDR optical system. *Here a beamsplitting prism breaks up the light into three parts, one for each sensor fitted with different filters. Designs that use absorptive filters like this one make inefficient use of light.*

HDR imaging with multiple same-time acquisitions

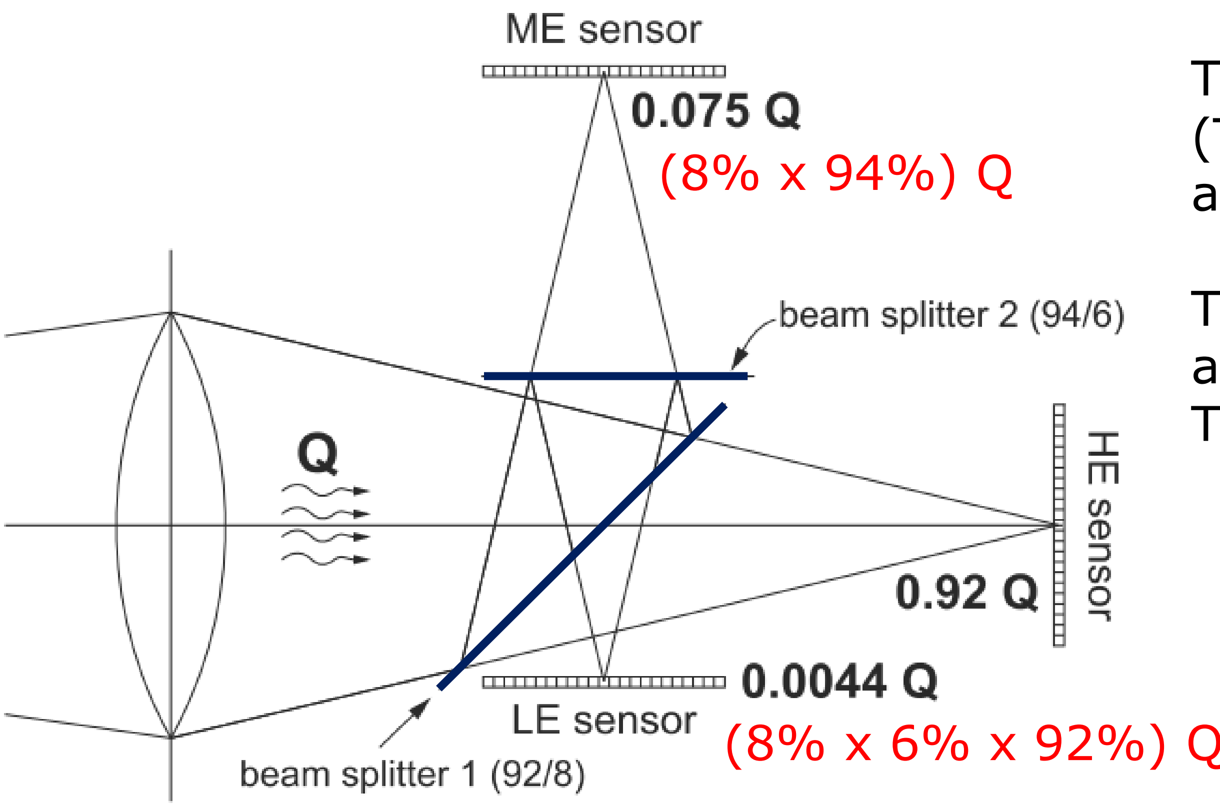

Figure 3: Illustration of our optical architecture. *We also use beamsplitters between the lens and sensors, but the key difference is that we re-use the optical path to improve our light efficiency. In the end, 99.96% of light entering the aperture arrives at the sensors. Light efficiency is important in all imaging applications.*

Transmittance/reflectance (T/R) ratio is a function of angle.

The first beam splitter is at a 45 deg angle and has T/R = 92/8

HDR imaging: merging LDR data

1. CALIBRATION (relative): The response of each LDR imager is determined via multiple expositions of the same subject with constant aperture, variable time.

- Value of pixel *Z* is a nonlinear function *f* of the *amount of integrated light* *X*: $Z = f(X)$
- *X* is the product between illuminance and exposure time: $X = E\,\Delta t$
- *f* is supposed to be *smooth* and *monotonic*
- f^{-1} is determined via MMSE on a set of experiments (next slide)

Response curve of a digital camera. 11 photographs taken at f/8 with times ranging from 1/30 to 30 s, in 1-stop increments. 45 pixel locations observed across the image sequence.

CCD imagers produce linear output, but the curve shows that the camera nonlinearly remaps the data, to mimic the response curves found in film.

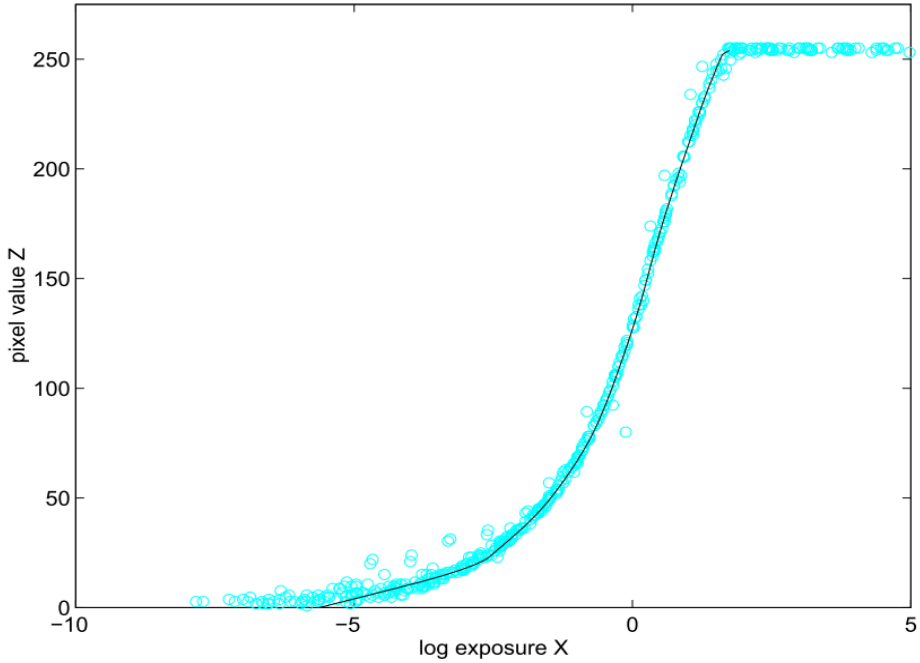

Debevec

HDR imaging: merging LDR data

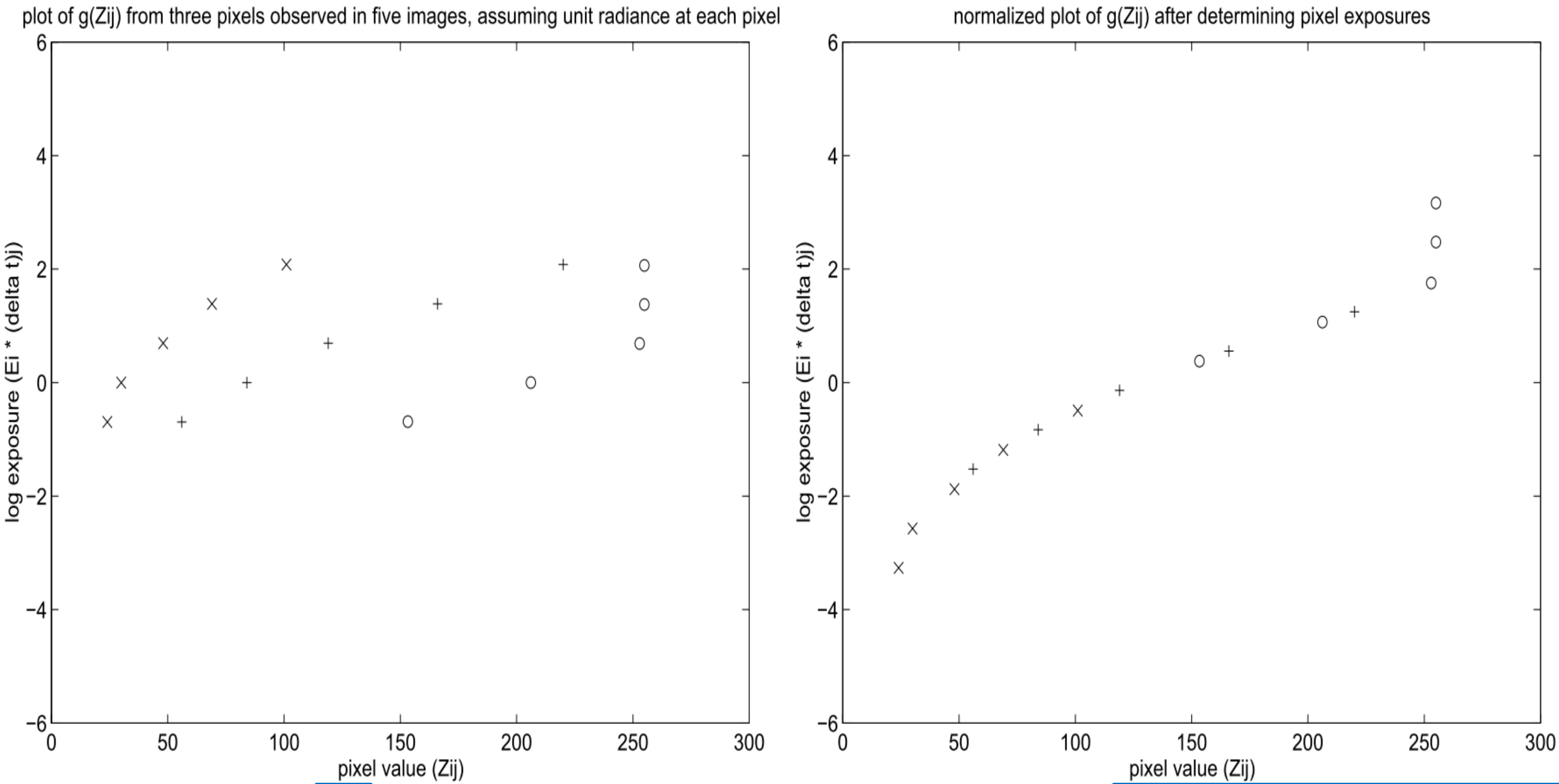

Figure 2: *In the figure on the left, the $\times$ symbols represent samples of the g curve derived from the digital values at one pixel for 5 different known exposures using Equation 2. The unknown log irradiance* $\ln E_i$ *has been arbitrarily assumed to be* 0. *Note that the shape of the g curve is correct, though its position on the vertical scale is arbitrary corresponding to the unknown* $\ln E_i$. *The* $+$ *and symbols show samples of g curve segments derived by consideration of two other pixels; again the vertical position of each segment is arbitrary. Essentially, what we want to achieve in the optimization process is to slide the 3 sampled curve segments up and down (by adjusting their* $\ln E_i$*'s) until they "line up" into a single smooth, monotonic curve, as shown in the right figure. The vertical position of the composite curve will remain arbitrary.*

HDR imaging: merging LDR data

2. DATA POOLING : The LDR contributions are mapped according to *f^-1* and combined with suitably shaped weights

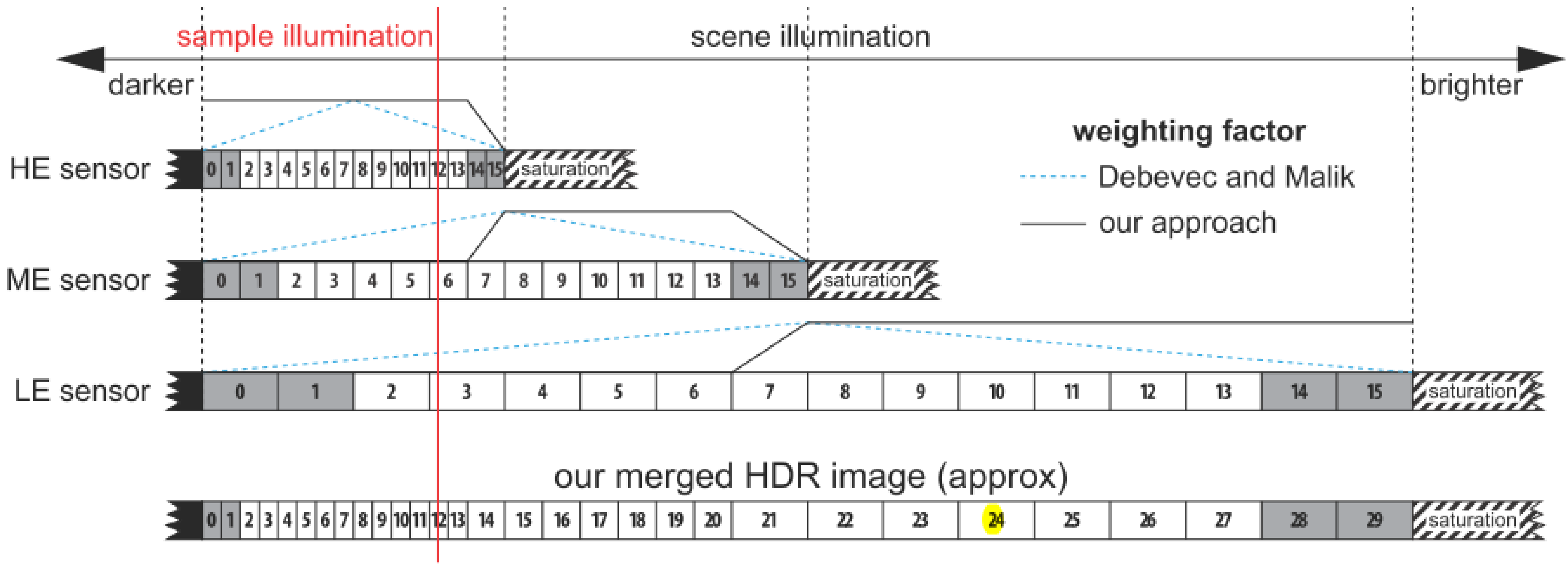

- (LDR images simplified to 4-bit sensors)
- OLD triangular: there are non-zero contributions from the LE sensor at low brightness values (like the sample illumination level indicated), even though the data from the LE sensor is coarsely quantized
- NEW trapezoidal: use data from the higher-exposure sensor as much as possible and blends in data from the next darker sensor when near saturation.

Sequential HDR imaging: merging LDR data

Double-exposure approach: z03_HDR_sequential....pdf

In case of moving image parts: *deghosting* algorithms [z03_HDR_deghosting]

→ *"Photographing the world as we see it with our own eyes"*

→ Mixed same-time / sequential approach: Milanfar 2020 talk

→ Improve color quality: z03_sens1_QuantumDots

Scientific and industrial **x-ray** sensors

- X-ray beam alignment in synchrotron radiation facilities [Hamamatsu]

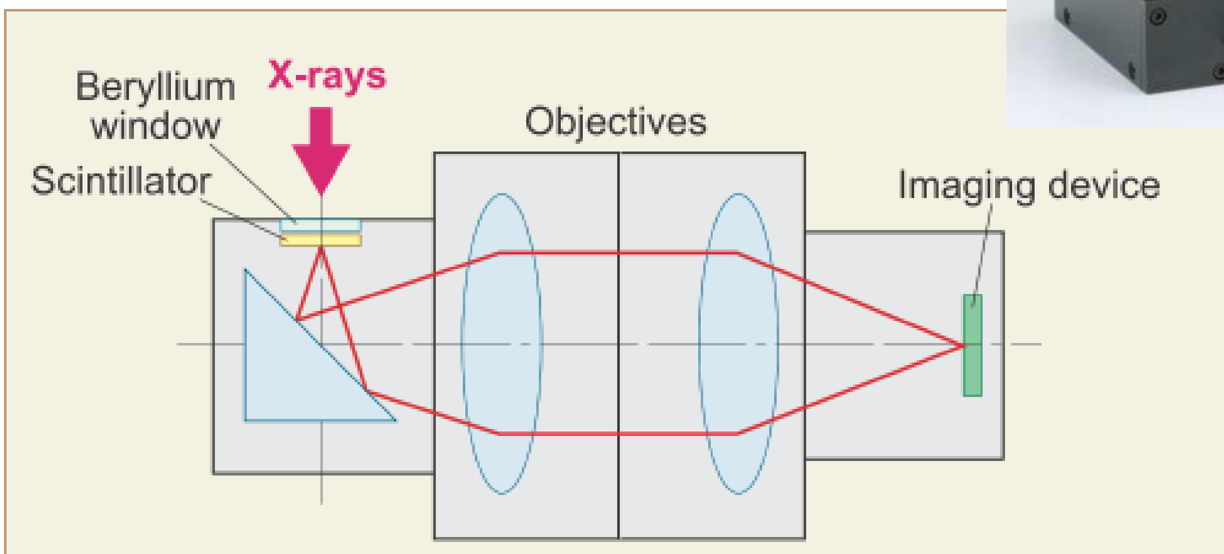

The irradiated X-ray is converted to visible light and conducted to the lens bended 90 degrees by L-shaped mirror in order to reduce the X-ray damage onto the digital camera.

Entrance window: Be is used for low-energy X-rays; Al, Fe, Cu for increasing energy levels

- Non-destructive testing [see leaflet: Dalsa]

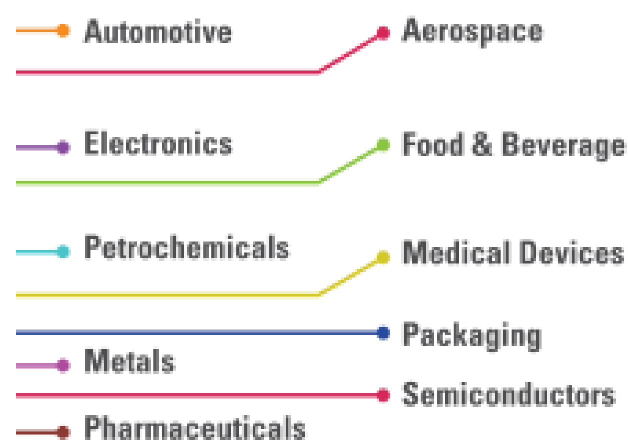

Medical x-ray sensors

IMAGING DETECTOR SPECIFICATIONS

Detector Array	Full field, single VHD CCD
Active Image Size	43 cm x 43 cm (17" x 17")
Pixels	4,128 x 4,128 (16 Megapixel)
Pixel Size (element pitch)	108 microns
Spatial Frequency (Nyquist)	4.6 lp/mm
Bit Depth	14 bit capture
Fill Factor	100%
AEC	3 field
Preview Image	Less than 6 seconds
Processed Image Display	Approximately 10 seconds
Acquisition Cycle Time	Immediately upon display of previous image

Plenoptic imaging

A.k.a. **Light-field** imaging

CONCEPT: collect information also about the ***direction*** of the light rays impinging on the sensor

Trade-off resolution with direction info: each pixel is no longer associated to rays hitting a position in the sensor from ‘all’ directions, but to a single ray → more pixels are needed for each image position

Applications:

- *Depth estimation*
- *Synthetic refocusing* after image acquisition
- *Computer vision* (see Sec.VII in paper below)

→ z03_LightField_Overview (theory, acquisition, super-resolution, depth estimation, compression, display, applications)

Plenoptic imaging

[Adelson 92]

The rich information available in (d) is lost on the sensor, where all light rays reaching a position from different directions are accumulated

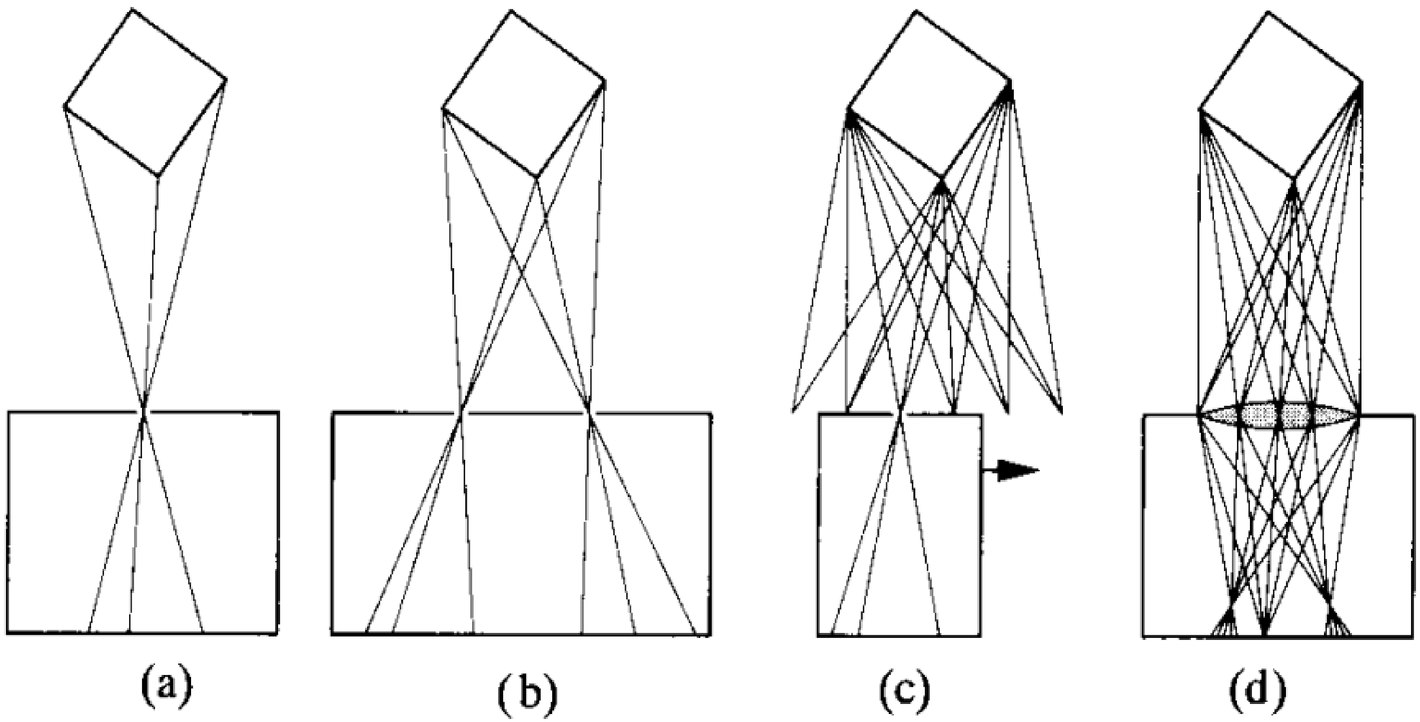

Fig. 2. (a) Pinhole camera forms an image from a single viewpoint; (b) in a stereo system, two images are formed from different viewpoints; (c) in a motion parallax system, a sequence of images are captured from many adjacent viewpoints; (d) a lens gathers light from a continuum of viewpoints; in an ordinary camera these images are averaged at the sensor plane.

Plenoptic imaging

By the way, note defocused object points in (d), not present in pinhole camera

In a conventional camera, depth-of-field is related to aperture

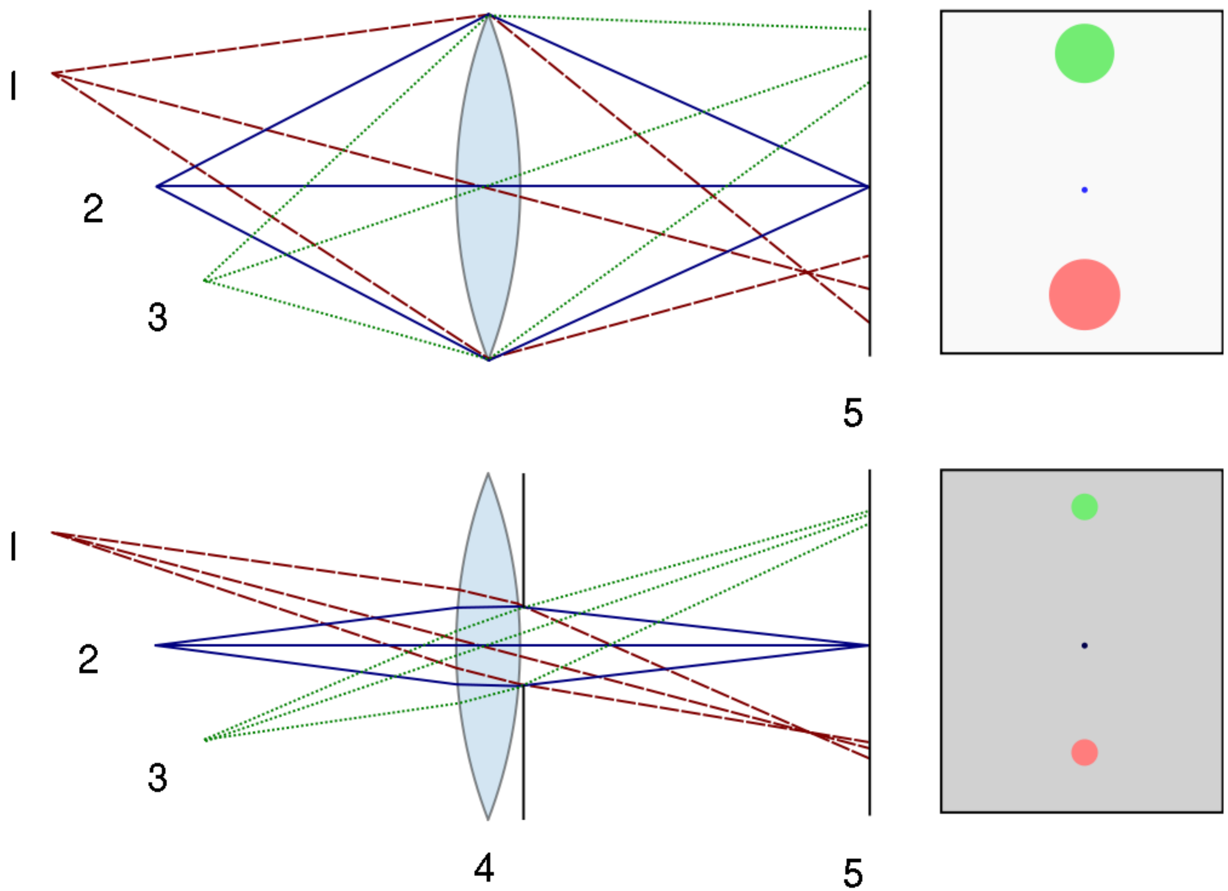

Circles of confusion

Plenoptic imaging

Fig. 3. Principle of single lens stereo: (a) In-focus point object forms a point image; (b) near object; (c) far object forms a blurred image; (d) with an eccentric aperture, the image of the in-focus object retains its position, but the images of the near or far objects (e) and (f), are displaced to the right or left.

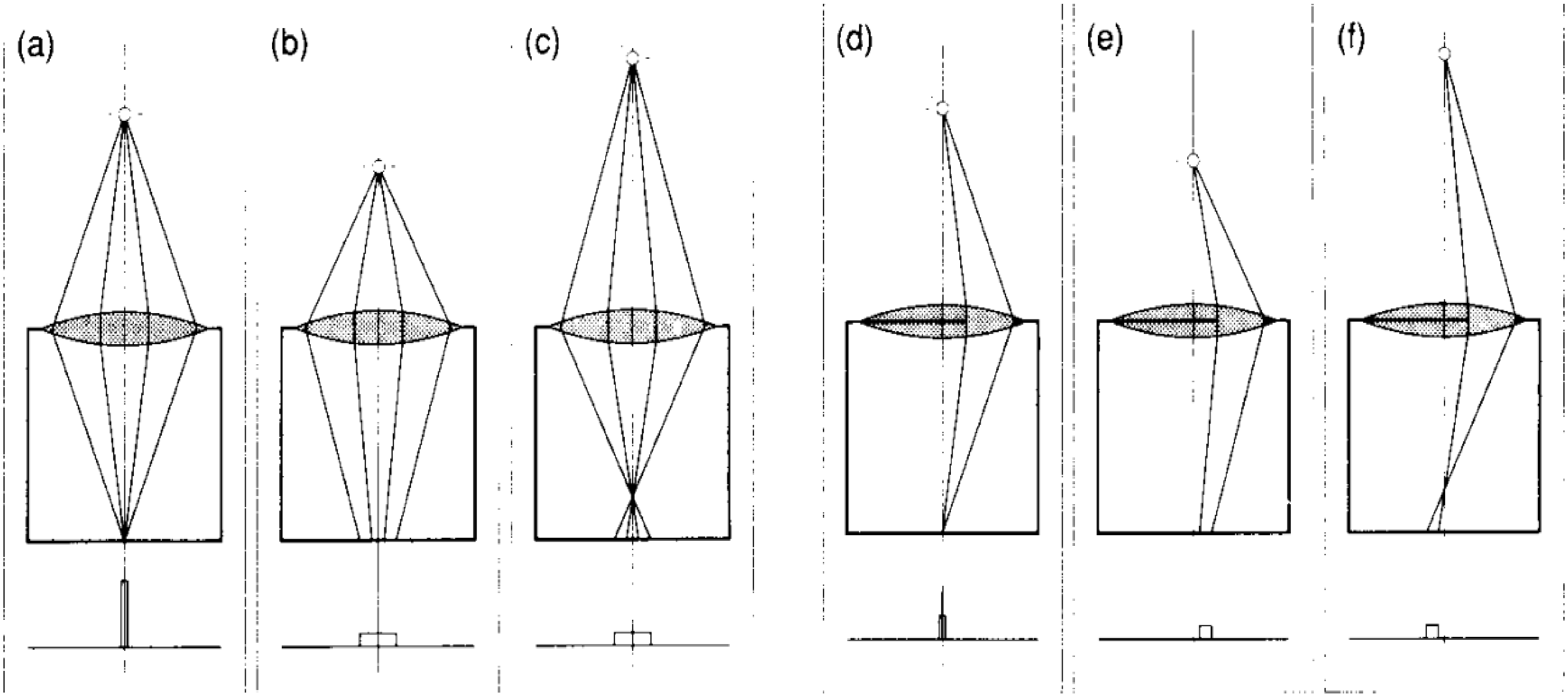

Plenoptic imaging

Replace the sensor in Fig.3 a/b/c with an array of pinhole cameras

Three lower-resolution images are formed: r, s, t. In-focus objects are aligned in the three images (a); close (b), and distant (c) objects are differently shifted. I.e., info about angle of ray incidence is preserved.

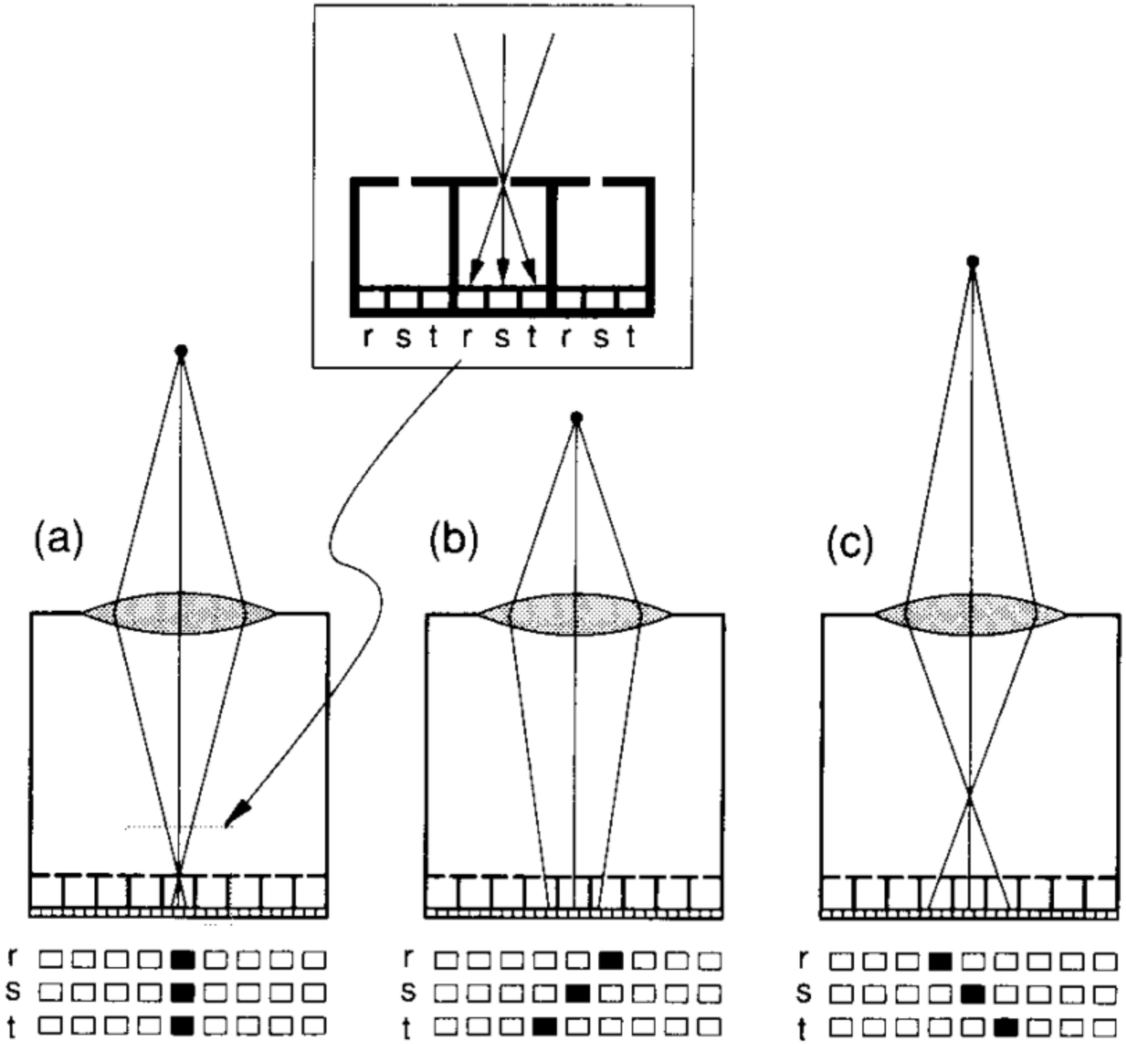

Fig. 5. Array of miniature pinhole cameras placed at the image plane can be used to analyze the structure of the light striking each macropixel.

Plenoptic imaging

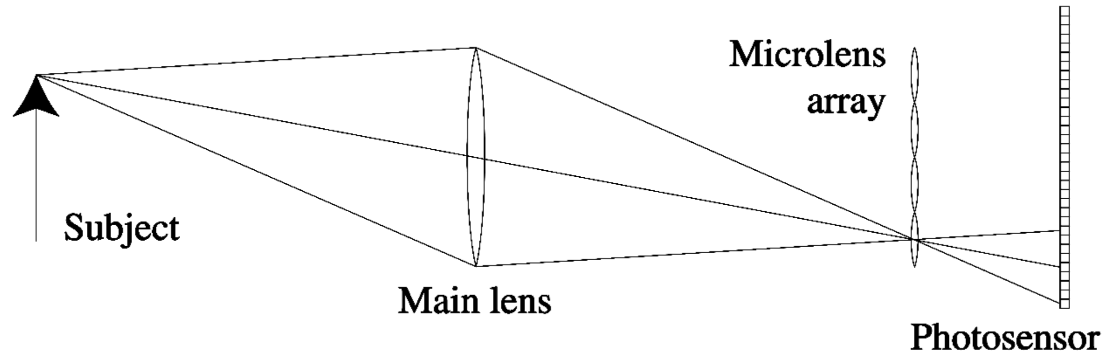

[RenNg05]

With microlens array (out of scale drawing)

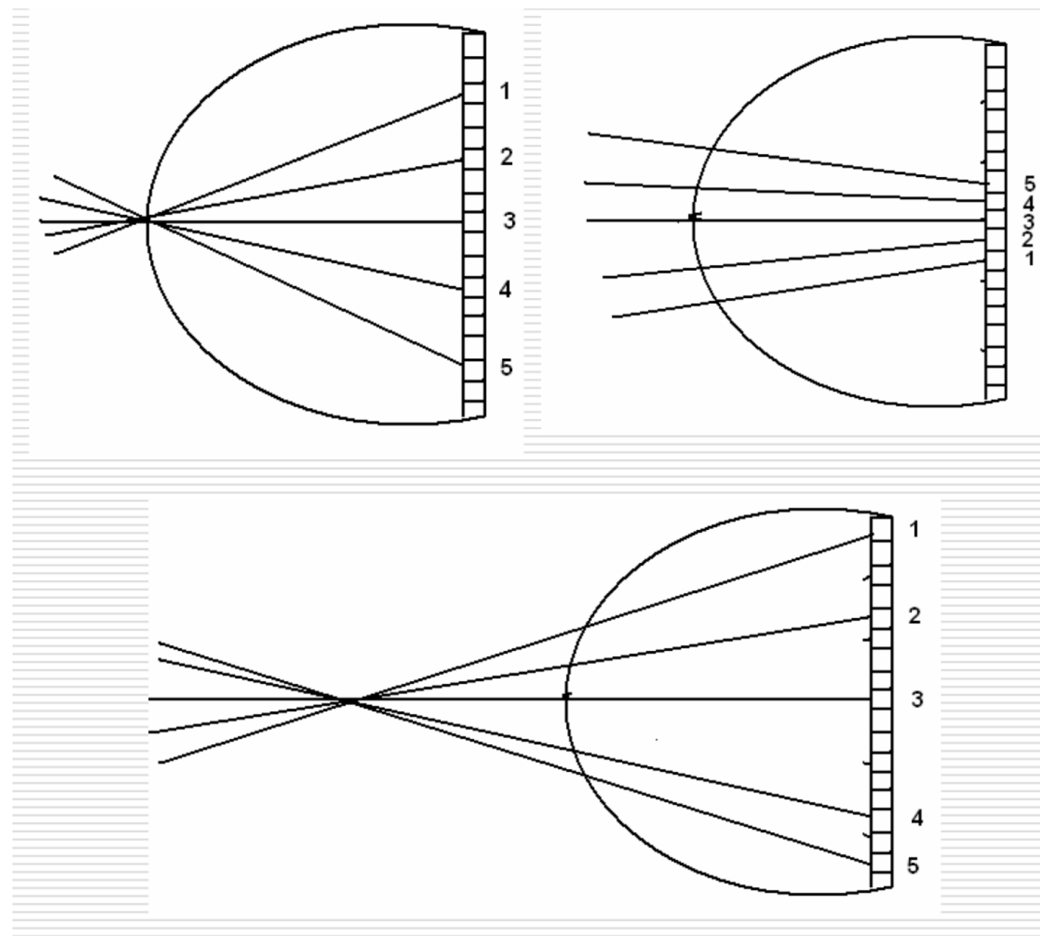

re-sorting pixels permits synthetic refocusing or generation of a stereoscopic image pair

Plenoptic imaging

Example Image

Image taken by Todor Georgiev, Adobe Systems, with his plenoptic camera.

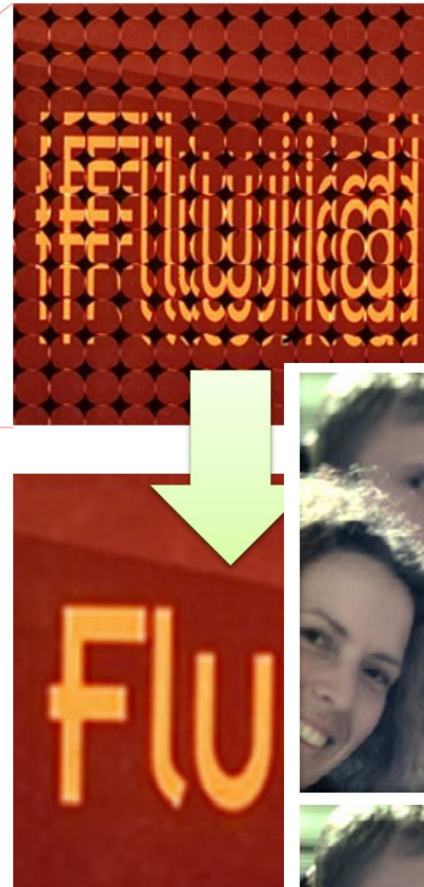

Synthetic refocusing

ng

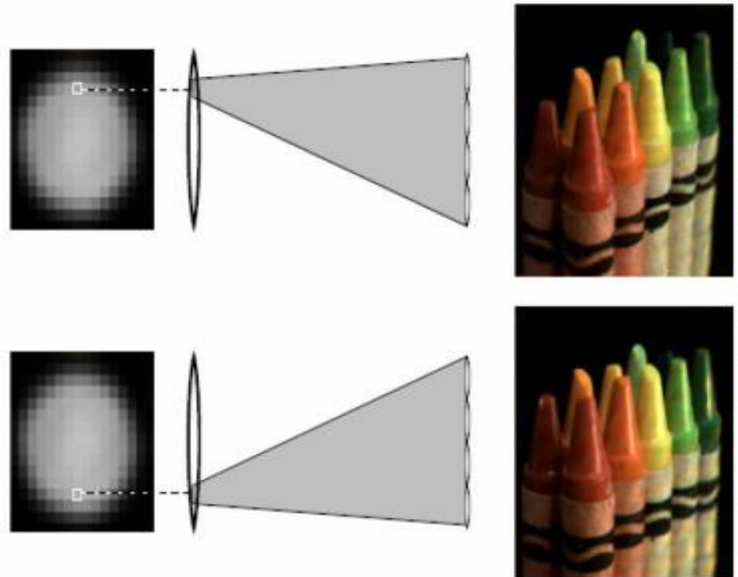

note perspective change (like in *eccentric aperture* approach seen earlier)

By performing a displacement analysis on successive images obtained from horizontal and vertical pixels, a depth map can be formed.

Views along the vertical and horizontal axes

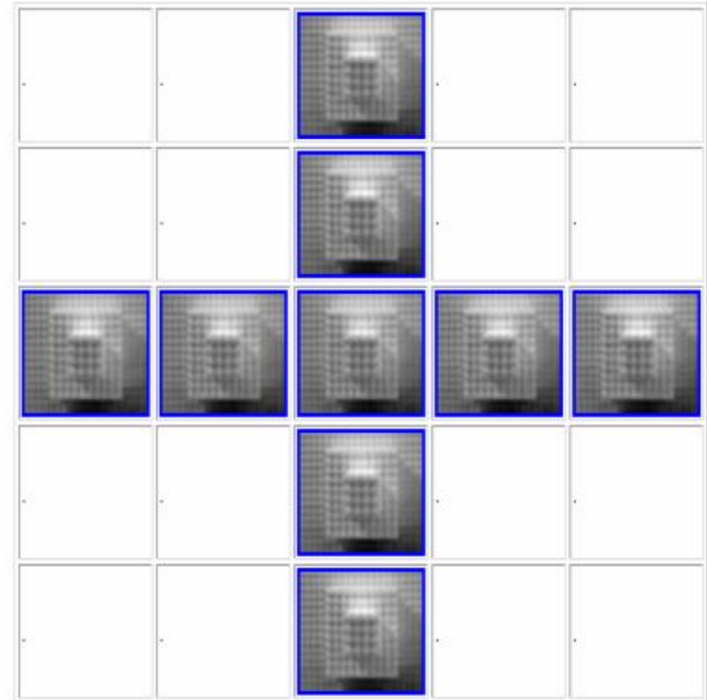

3D Recovery

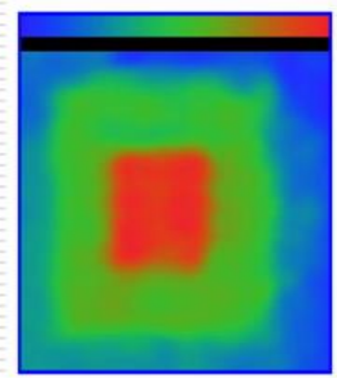

Depth map of a Lego pyramid

Lightfields and sw @ Stanford Univ.:
lightfield.stanford.edu/lfs.html
→ Chess → view online

www.raytrix.de
video tutorials and technology

Plenoptic imaging

Occlusion

Depth estimation with conventional stereo camera ∞

with Stereo Camera System

Red area can only be seen by left camera L. Therefore, no depth calculation possible in this area.

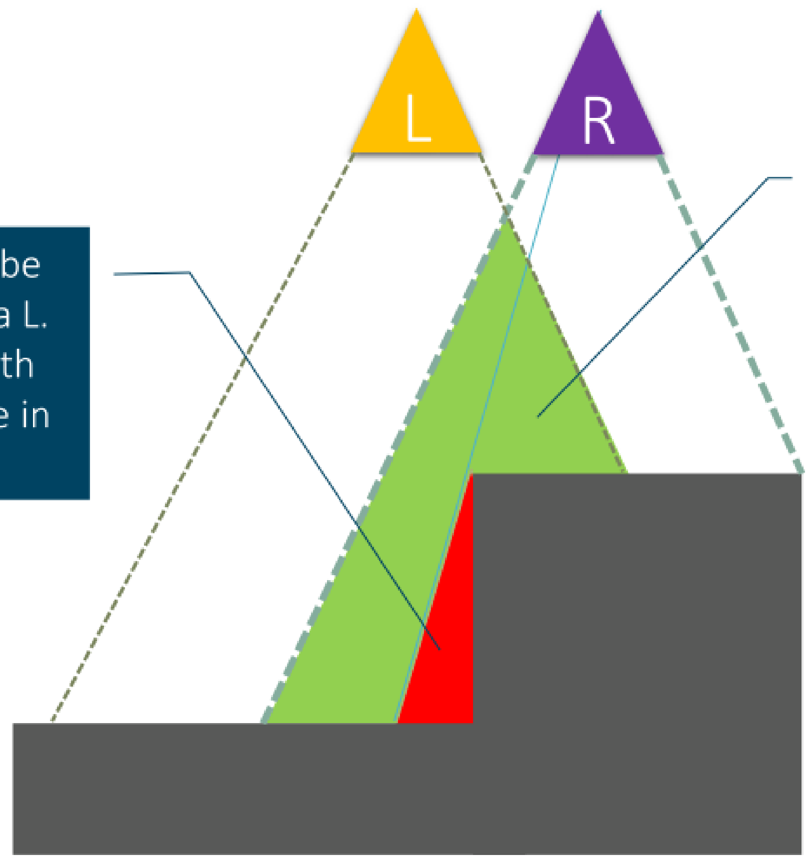

Depth estimation possible only in green area.

Plenoptic imaging

Occlusion

with Light Field Camera

No occlusion area in this example due to many micro cameras with small field of view

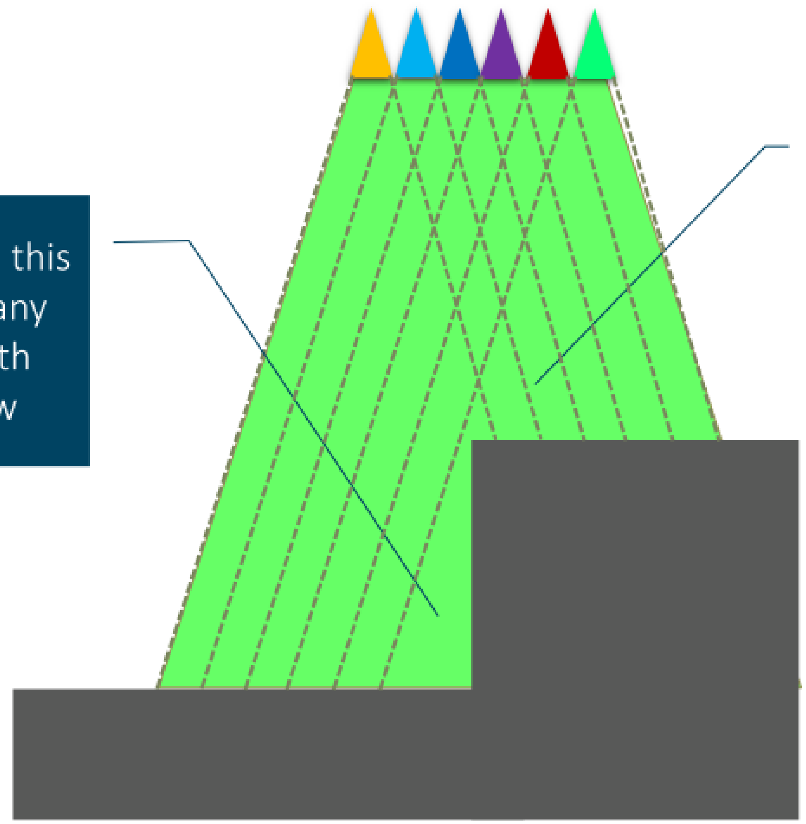

Depth estimation possible in green area

Multi-camera and **multi**-pixel

Multi-camera (2016)

16-sensors imaging: *Light L16* camera

- 50 Mpx interpolated images *or*
- synthetic 28-150 zoom *or*
- HDR imaging *or*
- select focus after shooting

Multi-camera smartphones:

- same sensors, different lenses (standard and wide-angle)
- high- and low-sensitivity sensors pair → HDR
- color sensor + b/w sensor for fine details
- Depth-dedicated sensors through stereo or ToF

Dual-pixel sensors:

- improved **autofocus**, and more

→ z03_DualPix_Modeling_Defocus
→ z03_DualPix_2017

(ISSCC 2023: **4**-Photodiode 50Mpx CMOS Sensor, 0.98e- Noise and 20Ke- Capacity)

3D imaging (even in your phone): **Time of Flight** (ToF)

May be used e.g. to blur the background in portraits (*bokeh* effect)

Used at first in front camera to help user identification

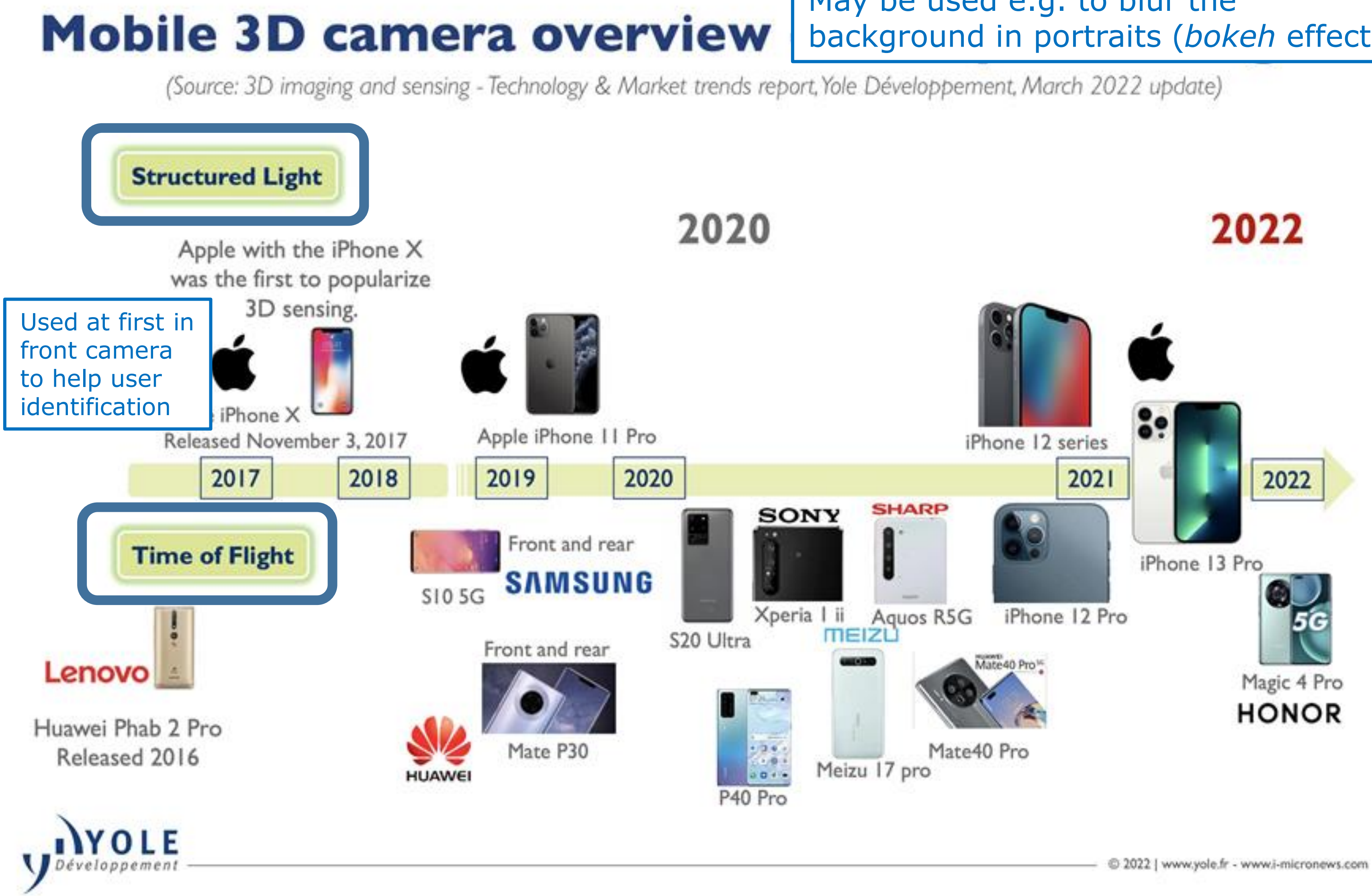

3D imaging: Time of Flight (ToF)

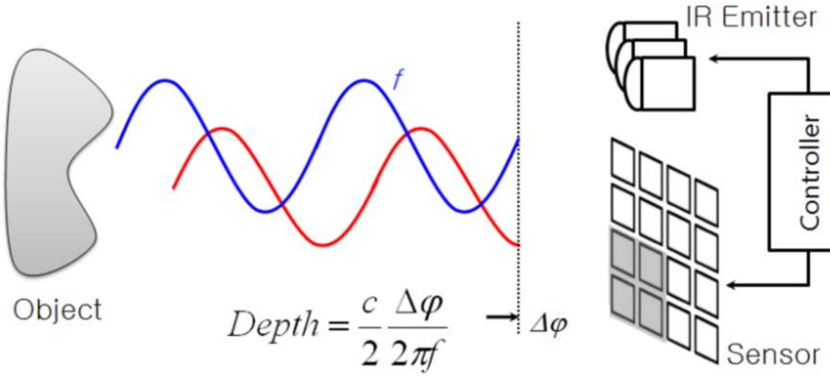

f: IR light modulation frequency
(e.g. 10 MHz)

Control signals measure fraction of light energy in [0, π] and in [π/2+0,π/2+π], respectively

$$\Delta\phi = \arctan\left(\frac{Q_3 - Q_4}{Q_1 - Q_2}\right)$$

Note: $\Delta\phi$ is a phase difference (radians)

$$d = \frac{c}{2f}\frac{\Delta\phi}{2\pi}.$$

Note: distance = flight path / 2

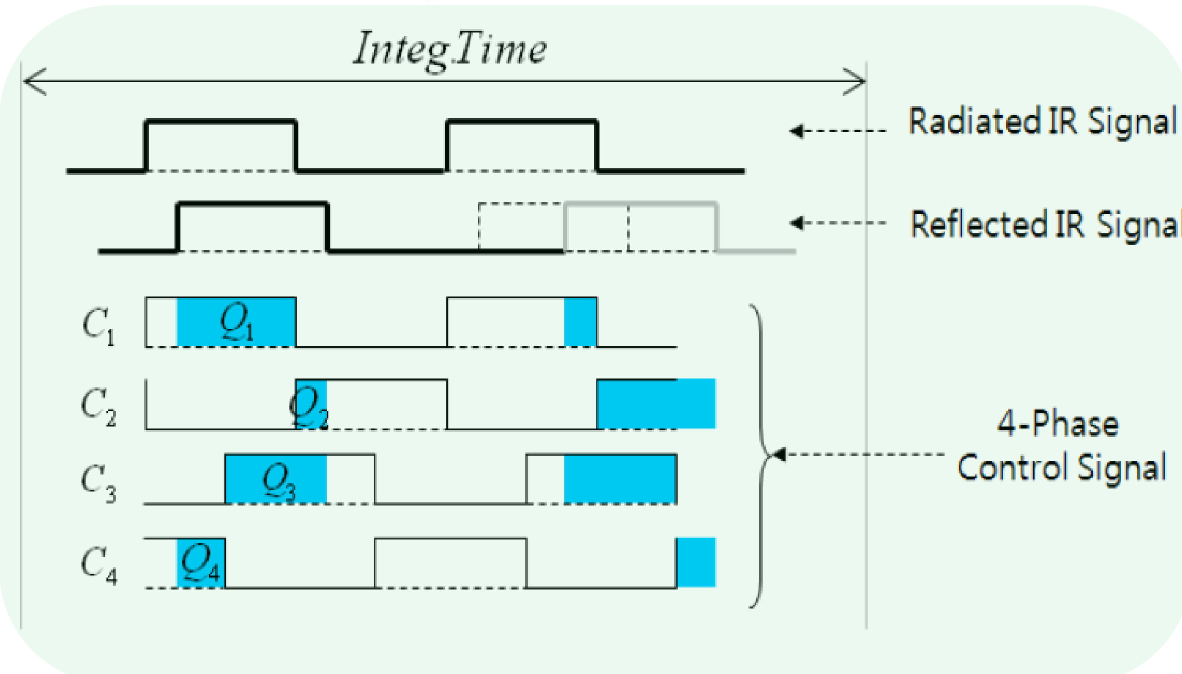

Fig. 1.2 Depth can be calculated by measuring the phase delay between radiated and reflected IR signals. The quantities Q_1 to Q_4 represent the amount of electric charge for control signals C_1 to C_4 respectively.

Max distance without phase ambiguity is $d = c/2f = \lambda/2$
(e.g. 3*10^8/(2*10^7) = 15m

Range can be extended using amplitude info to *unwrap* the phase

3D imaging: Time of Flight (ToF)

→ z03_ToFcamera_Infineon-REAL3
→ z03_ToFcamera_Theory
→ z03_ToF_Metalenses

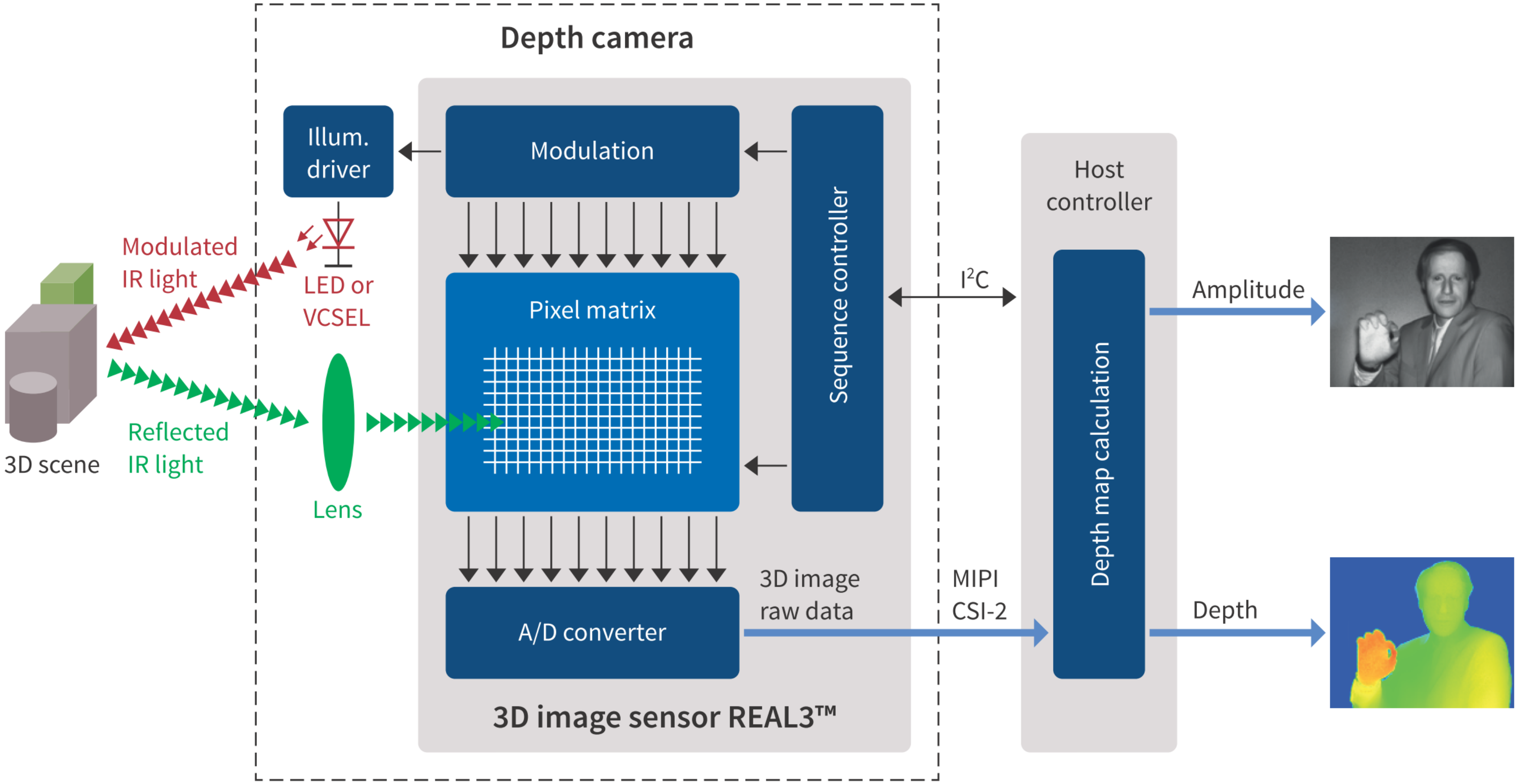

Multispectral and Hyperspectral imaging

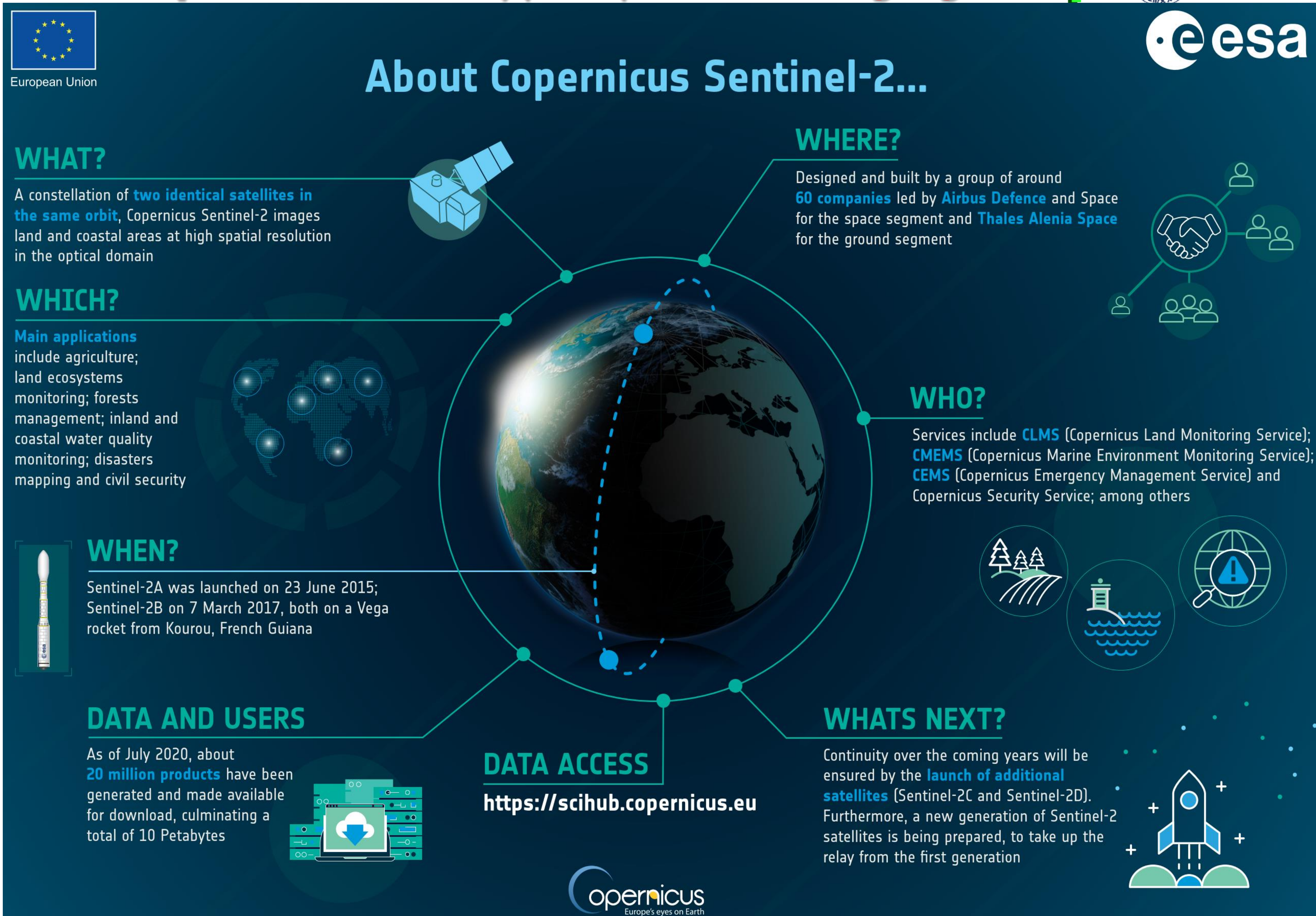

Multispectral and Hyperspectral imaging

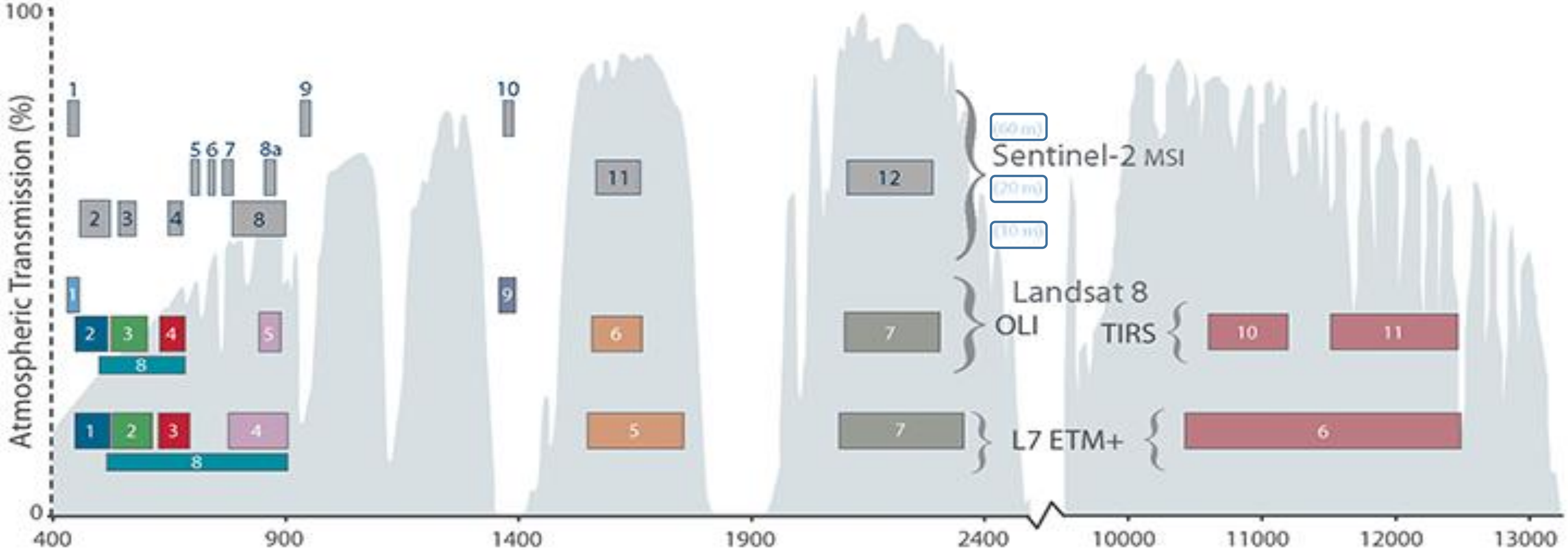

Band	Sentinel-2A MSI Spectral region	 Wavelength range (nm)	 Resolution (m)	Landsat 8 OLI Spectral region region	 Wavelength range (nm)	 Resolution (m)
B1				Blue	435–451	30
B2	Blue	458–523	10	Blue	452–512	30
B3	Green peak	543–578	10	Green	533–590	30
B4	Red	650–680	10	Red	636–673	30
B5	Red edge	698–713	20	NIR	851–879	30
B6	Red edge	733–748	20	SWIR1	1566–1651	30
B7	Red edge	773–793	20	SWIR2	2107–2294	30
B8	NIR	785–899	10			
B8A	NIR narrow	855–875	20			
B11	SWIR	1565–1655	20			
B12	SWIR	2100–2280	20			

VNIR: Visible and Near InfraRed
SWIR: Short Wave InfraRed

Multispectral and Hyperspectral imaging

Spectral signatures of targets are very diverse
→ dense spectral sampling is needed
→ hyperspectral sensors

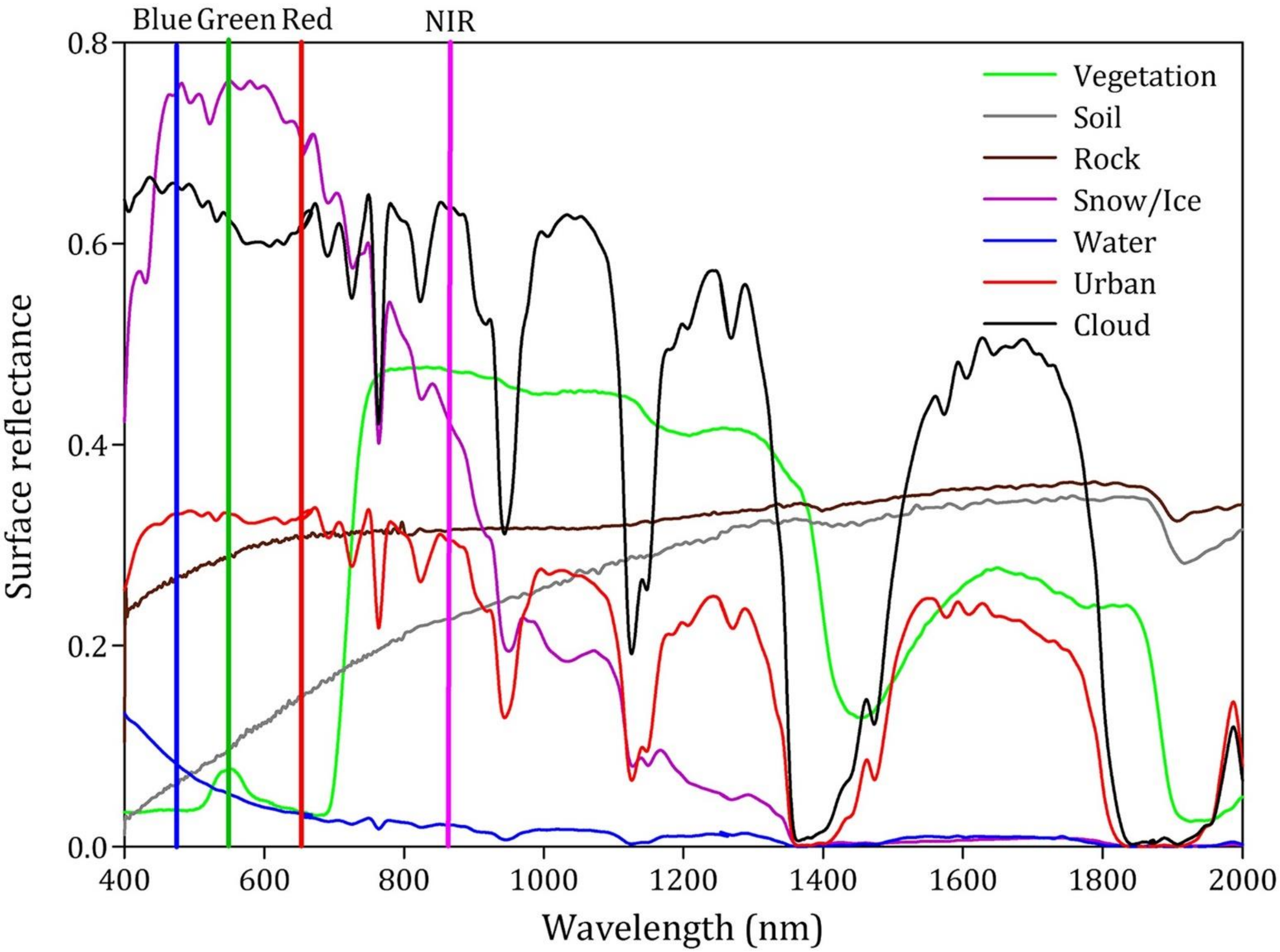

Multispectral and **Hyperspectral** imaging

PRISMA mission (ASI)

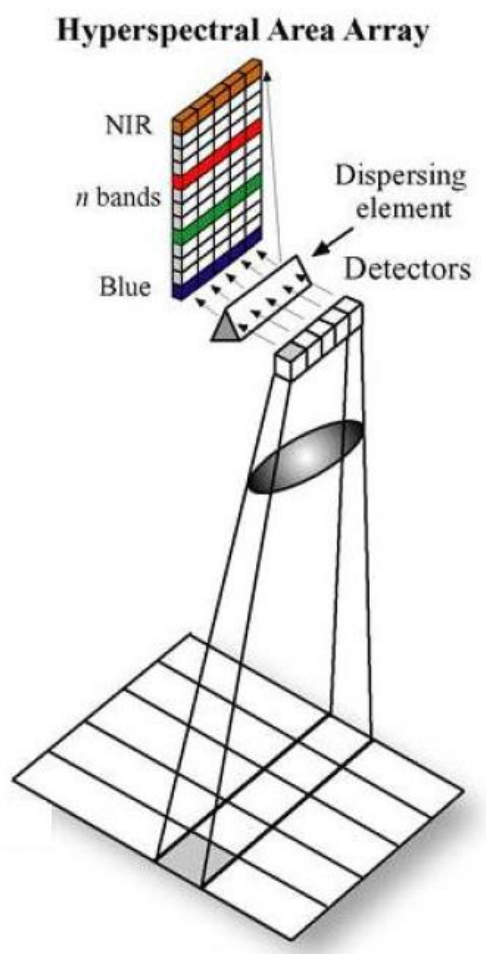

Pushbroom scanning and prism-based spectral analyser

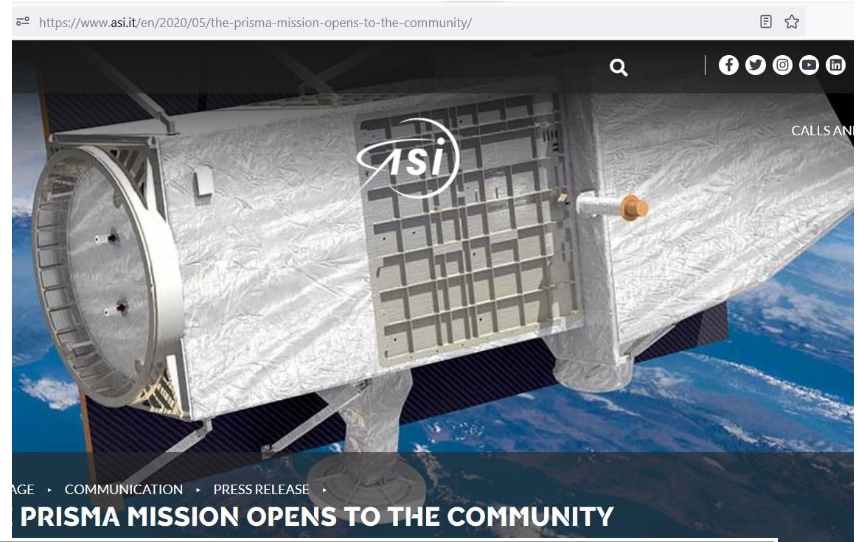

Swath / FOV	30 km / 2.77°
Ground Sampling Distance (GSD)	Hyperspectral: 30 m / PAN: 5 m
Spectral Range	VNIR: 400 – 1010 nm SWIR: 920 – 2505 nm PAN : 400 – 700 nm
Spectral Width (FWHM)	≤ 12 nm
Radiometric Quantization	12 bit
VNIR SNR	> 200:1
SWIR SNR	> 100:1
PAN SNR	> 240:1
MTF@ Nyquist freq.	VNIR/SWIR along track > 0.18 VNIR/SWIR across track > 0.34 PAN along track > 0.10 across track >0.20
Spectral Bands	66 VNIR / 173 SWIR
Data processing	Lossless compression with compression factor 1.6 Near lossless compression

Multispectral and **Hyperspect**

PRISMA mission (ASI)

Soil and Vegetation Components for Precision Agriculture

EO Products	Description
CLAY	Percentage of clay in the first 30 cm of soil
SILT	Percentage of silt in the first 30 cm of soil
SAND	Percentage of sand in the first 30 cm of soil
SOC	Percentage of organic carbon in the first 30 cm of soil

EO Products	Description
LAI	Leaf Area Index
Cab	Chlorophyll a and b Content of in leaves per unit of area
FPAR	Fraction of photosynthetically active radiation absorbed by vegetation cover

EO Products	Description
YLD	Crop production
QN	Content of nitrogen in the aboveground biomass
GN	Nitrogen content in grain
Nres	nitrate nitrogen (NO3-N-) in the soil at the end of crop cycle

Soil contamination – heavy metal

Spectral Library 110 samples

laboratory concentration (ppm) & ASD spectral measurements

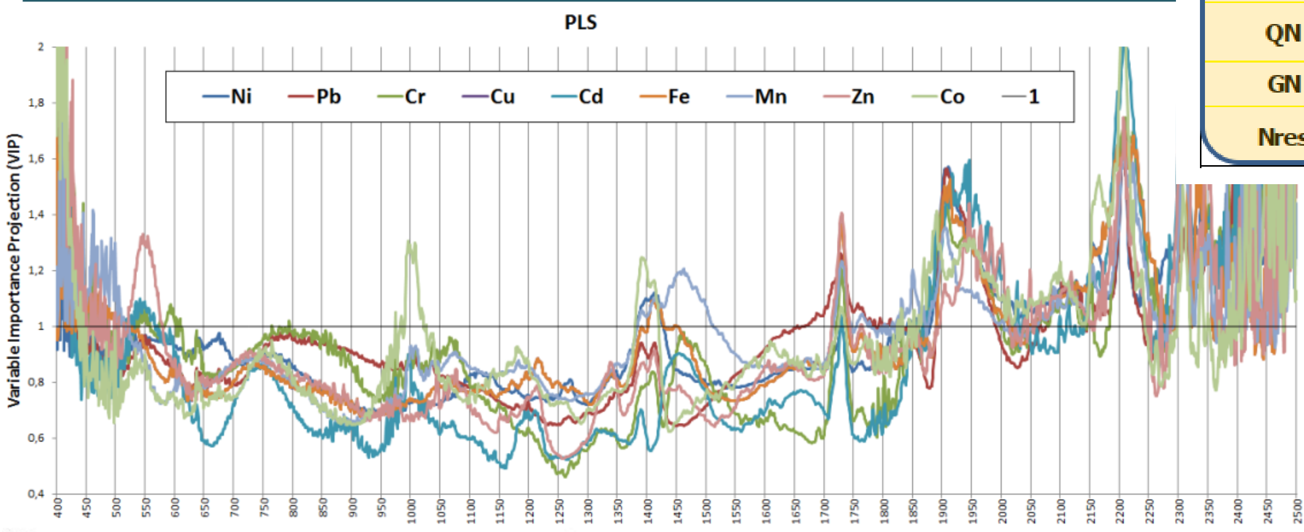

→ z03_Hyperspectral_ Imaging